# Real-time monitoring of peptide grafting onto chitosan films using capillary electrophoresis

Danielle L Taylor, Joel J Thevarajah, Diksha K Narayan, Patricia Murphy, Melissa M Mangala, Seakcheng Lim, Richard Wuhrer, Catherine Lefay, Michael D O'connor, Marianne Gaborieau, et al.

▶ **To cite this version:**

Danielle L Taylor, Joel J Thevarajah, Diksha K Narayan, Patricia Murphy, Melissa M Mangala, et al.. Real-time monitoring of peptide grafting onto chitosan films using capillary electrophoresis. Analytical and Bioanalytical Chemistry, 2015, 407 (9), pp.2543 - 2555. 10.1007/s00216-015-8483-y . hal-04036786

**HAL Id: hal-04036786**
**https://hal.science/hal-04036786**

Submitted on 20 Mar 2023

**HAL** is a multi-disciplinary open access archive for the deposit and dissemination of scientific research documents, whether they are published or not. The documents may come from teaching and research institutions in France or abroad, or from public or private research centers.

L'archive ouverte pluridisciplinaire **HAL**, est destinée au dépôt et à la diffusion de documents scientifiques de niveau recherche, publiés ou non, émanant des établissements d'enseignement et de recherche français ou étrangers, des laboratoires publics ou privés.

This version of the article has been accepted for publication, after peer review and is subject to Springer Nature's AM terms of use, but is not the Version of Record and does not reflect post-acceptance improvements, or any corrections. The Version of Record is available online at: http://dx.doi.org/10.1007/s00216-015-8483-y

# Real-time monitoring of peptide grafting onto chitosan films using capillary electrophoresis

Danielle L. Taylor[#],[1,2] Joel J. Thevarajah[#],[1,2] Diksha K. Narayan,[1,2,3] Patricia Murphy,[1,3] Melissa M. Mangala,[1,3] Seakcheng Lim,[1,3] Richard Wuhrer,[4] Catherine Lefay,[5] Michael D. O'Connor*,[1,3] Marianne Gaborieau*,[1,2] Patrice Castignolles[2]

1 University of Western Sydney, Molecular Medicine Research Group, Parramatta 2150 / Campbelltown 2560, Australia

2 University of Western Sydney, Australian Centre for Research on Separation Sciences (ACROSS), School of Science and Health, Parramatta 2150, Australia

3 University of Western Sydney, School of Medicine, Campbelltown 2560, Australia

4 University of Western Sydney, Advanced Materials Characterisation Facility (AMCF), Parramatta 2150, Australia

5 Aix-Marseille Université, CNRS, ICR UMR 7273, 13397 Marseille, France

[#]Joel Thevarajah and Danielle Taylor contributed equally

* corresponding authors: (M. O'Connor) e-mail m.oconnor@uws.edu.au, tel +61 2 4620 3902, fax +61 2 4620 3890; (M. Gaborieau) e-mail m.gaborieau@uws.edu.au, tel +61 2 9685 9905, fax +61 2 9685 9905

## Abstract

Chitosan being antimicrobial and biocompatible is attractive as a cell growth substrate. To improve cell attachment RGDS peptides (arginine - glycine - aspartic acid - serine) were covalently grafted to chitosan films, through the widely used coupling agents EDC-HCl (1-ethyl-3-(3-dimethylaminopropyl)carbodiimide) and NHS (N-hydroxysuccinimide), via the carboxylic acid function of the RGDS molecule. The grating reaction was monitored, for the first time, in real time using free-solution capillary electrophoresis (CE). This enabled fast separation and determination of the peptide and all other reactants in one separation with no sample preparation. Covalent RGDS peptide grafting onto the chitosan film surface was demonstrated using solid-state NMR of swollen films. CE indicated that oligomers of RGDS, not simply RGDS, were grafted on the film, with a likely hyperbranched structure. To assess the functional properties of the grafted films cell growth was compared on control and peptide-grafted chitosan films. Light microscopy and polymerase chain reaction (PCR) analysis demonstrated greatly improved cell attachment to RGDS-grafted chitosan films.

## Keywords

chitosan, peptide, capillary electrophoresis, solid-state NMR spectroscopy, retinal pigment epithelial cells

## Introduction

Chitin is the second most abundant polysaccharide in the world (by volume after cellulose) and is the main component extracted from discarded shells and gladii of crustaceans and molluscs; it is thus readily available, inexpensive and abundant.[1, 2] Chitosan is derived from the *N*-deacetylation of chitin. It can be dispersed in acidic media and easily cast into fibres, gels, beads, scaffolds, nanoparticles and films.[3] Chitosan exists as a linear copolymer of *β*-[1,4]-linked 2-acetamido-2-deoxy-D-glucopyranose and 2-amino-2-deoxy-D-glucopyranose (monomer units bearing different functional groups, see Fig. S-1 in Electronic Supplementary Material).[4] Its antifungal [5], antibacterial [6] and low immunological [7] properties make it promising for various biomedical applications including as a substrate for culture of stem cells [8-11] and other cell types.[12]

Cell survival and appropriate functioning are intimately linked with cell attachment to cell type-specific extracellular matrix proteins.[13] For example, biomaterials used in prostheses, vascular grafting and artificial skin require substantial anchorage and adhesion to cells.[14] The peptides RGD (arginine - glycine – aspartic acid) and RGDS (arginine - glycine – aspartic acid – serine) are fibronectin mimetics that have been extensively used in cell attachment studies due to their ability to increase and mediate cell adhesion on biomedical components. When grafted to a silicone surface, RGD was shown to trigger similar cell attachment as the whole fibronectin protein.[15] Short peptides containing the tri-amino sequence RGD are thus cheaper substitutes for fibronectin when attempting to produce cell attachment to artificial surfaces. The RGD sequence acts as a ligand for cell surface integrin receptors as shown through their grafting on the thermoresponsive poly(*N*-isopropylacrylamide-*co*-*N*-acryloxysuccinimide).[16] Covalent grafting of RGD peptides can occur through amidification of the amine at the N-terminus of the peptide with the succinimide group of the corresponding co-monomer. In the case of chitosan films, grafting with the fibronectin protein (containing the RGDS sequence) has been achieved by

amidification (or esterification) of the protein's carboxylic acid groups onto the amine (or alcohol) moieties on the chitosan surface via the coupling agents 1-ethyl-3-(3-dimethylaminopropyl)carbodiimide (EDC-HCl) and N-hydroxysuccinimide (NHS)[17]. The resulting covalently grafted fibronectin-chitosan surface promoted the adhesion and proliferation of SaOs-2 human osteoblast-like cells compared to bare chitosan films. This grafting method has been applied to RGD or RGDS, but usually to graft the peptide through its amine (not carboxylic acid) functional group onto carboxylic acid functional groups of the substrate, requiring a chemical modification of chitosan [11]. The use of EDC / NHS appears more straightforward, and thus preferable, in comparison to grafting through the photochemical activation of RGDS [18-20] or the thiolation reaction using *N*-succinimidyl-3-(2-pyridyldithio)propionate.[21] Grafting with EDC-HCl and NHS is often assumed to lead to quantitative grafting of RGD(S).

Knowledge of the grafting reaction enables adjustments to be made to the reaction time. Similarly, determination of the actual final peptide consumption enables adjustment of its initial concentration to avoid wastage. To analyze peptide grafting processes, appropriate determination of the reactants and products is necessary. For chitosan films the grafting process has previously been monitored by direct characterization of the grafted films. For example, amino acid analysis (AAA) has been used on a chitosan scaffold with peptide grafted from the chitosan amine [22], and also a carboxymethylated chitosan with peptide grafted from the carboxylic acid functional group introduced on the chitosan surface [23]. In the first of these studies, the yield of grafted peptide was not reported, with only the final peptide density on the surface reported. In the second study the yield of the grafted peptide was reported as 10 to 12 %.

Critically, the AAA method used in these two studies is tedious and incompatible with simple and/or high-throughput assessment of the grafting process. It should also be noted that RGDS grafting onto chitosan does not yield an imide bond [22] but rather an amide bond. As

an alternative to the AAA method, grafting of RGD onto chitosan via EDC-HCl and NHS has been assessed through the fluorescence of a model system containing RGD labeled with fluorescein isothiocyanate (FITC).[24] Unfortunately no comparison of the grafted RGD quantity to the RGD originally introduced was made in this study, so the kinetics and the extent of the reaction cannot be accurately assessed. Moreover, the presence of the bulky FITC groups could alter the grafting process mediated by EDC-HCl and NHS. This is particularly relevant for processes involving RGD(S) polycondensation described in this work.

Solid-state characterization can also be used to characterize the grafting process, but as with AAA it has specific limitations such as the inability to be performed in real time. As an alternative, the grafting process can be characterized indirectly by monitoring the disappearance of the peptide from the reactant solution. Indirect monitoring may not differentiate between covalent grafting and adsorption; however, adsorption experiments can be carried out in parallel to assess the extent of adsorption. Reverse-phase HPLC has been used to quantify GRGD grafting on chitosan, but the method was deemed as only semi-quantitative.[20] In contrast, capillary electrophoresis (CE) has never been applied to monitor peptide grafting. However, in other systems CE has been used extensively to characterize both cationic and anionic peptides and proteins with relatively high recovery.[25, 26] It can also be used as an indirect method to monitor reactions in real time.[27] Additionally, free-solution CE has a lower running cost and is more robust than common HPLC methods,[28] and allows characterization in complex matrices for example of polysaccharides without sample preparation, not even filtration [29] including for chitosan [30]. Therefore, free-solution CE (also known as capillary zone electrophoresis), was assessed here to test whether the real-time monitoring advantages of CE are suitable for monitoring peptide consumption during peptide grafting onto chitosan films.

The physical characteristics of chitosan films may affect the grafting process and the application properties of biomedical products. Solid-state NMR spectroscopy under magic-angle spinning (MAS) enabled the characterization of various properties of chitosan films (e.g., composition, mechanical strength, elasticity).[3, 31, 32] Additionally, $^{13}C$ and $^{15}N$ NMR spectroscopy was used to determine the average composition of the chitosan in terms of degree of acetylation.[31] $^{1}H$, $^{13}C$ and $^{15}N$ NMR spectroscopy, combined with X-ray scattering, was used to reveal the molecular origin of several properties of chitosan films (e.g., mechanical strength, elasticity) depending on the film preparation (e.g., casting from weak or strong acid solution, neutralization or not).[3]

A range of cell types are relevant to regenerative medicine applications, including ocular retinal pigment epithelium (RPE) that play a key role in the development of macular degeneration. In vivo, the RPE requires attachment to Bruch's membrane to provide key regulatory signals for RPE survival and function.[33] Transplantation of RPE from various sources, in conjunction with synthetic Bruch's membrane, is widely viewed as a promising and viable method to restore vision in patients with diseased RPE [33]. Importantly, the RPE is known to attach to extracellular matrix proteins such as fibronectin within Bruch's membrane,[34] thus allowing transmission of bioactive signals to enhance cell adhesion and survival.[35]

In this context we report a simple method to graft biologically-relevant peptides onto chitosan films, to monitor the grafting reaction with CE, and to characterize the films by solid-state NMR spectroscopy. In doing so we demonstrate a simple, inexpensive and widely applicable method to successfully generate cell-type specific substrates that promote cell attachment and proliferation for downstream cell culture and other biomedical applications (e.g., transplantation).

## Materials and Methods

**Materials**

Chitosan powder (medium molecular weight, lot number MKBH1108V, average degree of acetylation, DA, of 24 % of monomer units and viscosity of 563 cP in 1 % acetic acid), *N*-hydroxysuccinimide (NHS, 98 %), 1-ethyl-3-(3-dimethylaminopropyl)carbodiimide (EDC HCl, 99 %), trifluoroacetic acid (TFA, 99 %), dimethylsulfoxide (DMSO), sodium hydroxide pellets and adamantane (99 %) were purchased from Sigma-Aldrich. Glucosamine (GLcN, 1000 mg capsules, batch number 23249) was purchased from Health Care, Australia. Boric acid (98 %) and orthophosphoric acid (85 %) were purchased from BDH AnalR, Merck Pty Ltd. Acetic acid (AcOH, glacial, 99 %) and hydrochloric acid (32 %) were purchased from Unilab. Singly labelled $^{13}$C-labelled alanines (1-$^{13}$C, 2-$^{13}$C, 3-$^{13}$C; 99 %) were purchased from Cambridge Isotope laboratories, Inc. The peptide RGDS (97 %) was obtained from Auspep Pty Ltd, Australia. Phosphate buffered saline solution (PBS) at pH 7.4 was prepared by dissolving 8 g sodium chloride, 0.2 g potassium chloride, 1.44 g disodium hydrogen phosphate and 0.24 g potassium dihydrogen phosphate in 0.8 L MilliQ water, and titrating the solution with hydrochloric acid to pH 7.4. Sodium borate buffer (75 mM) was prepared from 0.5 M boric acid in MilliQ water, titrated to pH 9.20 with 10 M sodium hydroxide and diluted with MilliQ water. Sodium borate buffers were filtered with a Whatman (0.2 µm) or Millex GP syringe filter (0.22 µm). A 1.33 wt/vol% glucosamine solution in MilliQ water was prepared for a control experiment.

**Preparation of chitosan films**

Chitosan films were cast from acetic acid dispersion according to a protocol adapted from Gartner et al. [3]. A 1.7 wt% chitosan suspension in a 2 wt% acetic acid aqueous dispersion was produced by stirring for 5 days at room temperature in the dark. The dispersion was centrifuged at 1076 g and 23 °C for 1 h and the precipitate discarded before 10 mL aliquots of the suspension were cast in 9 cm diameter plastic Petri dishes at room temperature. The resulting chitosan films were clear, colorless and 20 to 40 µm thick (Fig. S-2).

**Peptide grafting onto chitosan films**

The grafting protocol was adapted from Cheng and Cao (Fig. S-3 in Electronic Supplementary Material).[19] Briefly, EDC-HCl (3 mg, 3.13 mM), NHS (2 mg, 3.48 mM) and peptide (RGDS, 1 mg, 0.46 mM) were stirred in 5 or 10 mL PBS for 15 min at room temperature (except for the films Grafted-18h and Grafted-18h-d, for which the reaction medium was stirred for 5 min). The mixture was then poured into a glass Petri dish (9 cm or 5 cm diameter for 10 mL or 5 mL reaction medium, respectively) containing 10 x 1 $cm^2$ chitosan films (total 10 $cm^2$) (Table 1) covered with Parafilm and placed on a shaker for up to 18 h at room temperature (shaking exposes both surfaces of the film to the reaction medium). Aliquots of 50 µL were removed from the reaction medium at the commencement of the reaction and at variable intervals and analyzed via CE within 15 min after removal. Chitosan films were subsequently rinsed with PBS and MilliQ water then left to dry and stored in a -20 °C freezer. In one control experiment (Control-NoFilm), no chitosan film was used and RGDS was grafted instead on glucosamine (0.74 M) with EDC-HCl and NHS, as described above for all parameters other than chitosan and glucosamine (Table 1).

**Monitoring peptide grafting via CE**

Free-solution CE experiments were carried out using an Agilent 7100 CE (Agilent Technologies, Waldbronn, Germany) instrument equipped with a diode array detector. Polyimide-coated fused silica high sensitivity capillaries (50 µm internal diameter) were purchased from Agilent. The electrolyte was sodium borate (75 mM, pH 9.2). The capillary (43.5 cm total length, 35 cm effective length) was pretreated by a 10 min flush with NaOH (1 M), and then 5 min successive flushes with NaOH (0.1 M), MilliQ water and sodium borate (75 mM, pH 9.2). The capillary surface was regenerated between separations through a 1 min flush with NaOH (1 M) then a 5 min flush with sodium borate (75 mM, pH 9.2). All injections were hydrodynamic, i.e., pressure (30 mbar) was applied for 10 s. Detection was set at 195 nm. Separation was obtained applying 30 kV at 25 °C. Each injected solution

contained 0.22 vol% DMSO as an electroosmotic flow marker. An oligoacrylate with a known separation [36] and a broad range of mobilities was injected to validate the capillary and the instrument before each session.

The peptide consumption was calculated by determining the area under the curve of the identified RGDS peak divided by the migration time at each time interval and then normalizing it to the area determined for the aliquot just before the peptide mixture was introduced to the chitosan films.

**Solid-state NMR spectroscopy**

Chitosan powder was packed as received from the manufacturer into a 4 mm outer diameter rotor (with 3 mm internal diameter), and 10 x 1 $cm^2$ films were stacked and rolled to be packed into a 4 mm outer diameter rotor (with 2.5 mm internal diameter). This method of rotor packing was used for Non-treated, Control-soaked, Neutralized, Ethanol-washed, Grafted-2h and Grafted-2h-d films. Grafted-18h-r1 films were cut into small circles using a hole punch and then stacked in a 4 mm outer diameter rotor (with 2.5 mm internal diameter). The 10 x 1 $cm^2$ fresh (wet) Grafted-18h films and control-soaked films were swollen with fresh PBS buffer by soaking for 1 hour, stacking and then rolling to be packed in a 4 mm outer diameter rotor (with 3 mm internal diameter). Additional PBS was added to the rotors and films were left to soak for a half hour.

The $^{13}C$ cross-polarization (CP) and $^{1}H$, $^{13}C$ single-pulse excitation (SPE) NMR spectra were recorded under magic-angle spinning (MAS) on a Bruker DPX200 spectrometer operating at 200 and 50 MHz Larmor frequencies for $^{1}H$ and $^{13}C$, respectively. A commercial double resonance probe supporting high-speed zirconia MAS rotors with a 4 mm outer diameter was used at a spinning frequency of 10 kHz. The $^{1}H$ MAS NMR spectra were recorded with a 3 s relaxation delay and 64 scans. For $^{13}C$ NMR experiments, $^{1}H$ decoupling was used during the acquisition. The $^{13}C$ CP-MAS NMR spectra [3] were recorded with a 2 ms contact time and a 5 s relaxation delay, 10,240 scans for the powder and 20,480 scans for

the films (Non-Treated, Control-Soaked, Neutralized, Ethanol-washed, Grafted-2h, Grafted-3h, Grafted-18h-r1). The $^{13}C$ SPE-MAS NMR spectra were recorded with a 5 s relaxation delay and 61,945 scans for the powder and the same films (102,400 scans for Grafted-18h-r1). The $^{13}C$ CP-MAS NMR spectra of swollen films were recorded with a 0.2 ms contact time and a 3 s relaxation delay, 56,896 scans for Control-soaked and 81,920 scans for Grafted-18h. The $^{13}C$ SPE-MAS NMR spectra of swollen films were recorded with a 3 s relaxation delay and 112,640 scans for Control-soaked and Grafted-18h. The $^{1}H$ and $^{13}C$ pulses were calibrated with adamantane and a mixture of 3 singly $^{13}C$ labelled alanines. The $^{1}H$ and $^{13}C$ chemical shift scales were externally referenced to tetramethylsilane (TMS) at 0.0 ppm using adamantane by setting the CH resonance to 1.64 and 38.5 ppm, respectively.[37]

**Cell Culture**

The ARPE-19 (retinal pigment epithelial) and FHL124 (lens epithelial) cell lines used here were obtained from the American Type Culture Collection, and all cell culture[38, 39] was performed in a Class II Biological Safety Cabinet (Gelaire, Sydney, Australia). Cultured cells were maintained in DMEM containing 10 % fetal bovine serum and 1x penicillin/streptomycin (Life Technologies, Australia) using a Heracell 150 $CO_2$ incubator set at 37 ºC with an atmosphere of 5 % $CO_2$ (ThermoFisher Scientific, Melbourne, Australia). Cells were passaged every 7 days as single cells using TrypLE (Life Technologies) and plated onto tissue culture plastic. For experiments, cells were plated at a density of $7x10^5$ in 24 well plates either onto tissue culture plastic, 1 $cm^2$ non-grafted chitosan film, or 1 $cm^2$ RGDS peptide-grafted chitosan film. Imaging was performed using an Olympus CKX41 inverted microscope, digital camera (Olympus, Melbourne, Australia) and QCapture Pro™ 6 software (QImaging, Sydney, Australia).

**RNA Purification and PCR**

RNA was harvested from cells using an ISOLATE RNA Purification Kit (Bioline, Australia) and complementary DNA (cDNA) produced via reverse transcription (Bioline).

Polymerase chain reaction (PCR)[38, 39] was performed for key transcription factors known to be expressed by ARPE-19 cells; PAX6 and MITF using the following primers: PAX6 Fwd CCCCACATATGCAGACACAC, PAX6 Rev TCACTTCCGGGAACTTGAAC; MITF Fwd CGAAAGTTGCAACGAGAACA, MITF Rev GAGCCTGCATTTCAAGTTCC. PCR amplification was performed using an Eppendorf AG thermocycler (Hamburg, Germany) and involved 45 cycles of: 95 ºC, 30 seconds; 55 ºC, 30 seconds; and 72 ºC, 45 seconds. PCR products were separated on a 2 wt/vol% agarose/TAE gel and imaged via a GelDock transilluminator (BioRad, Australia).

## Results and Discussion

### Monitoring the grafting by free-solution CE

The peptide RGDS was grafted onto chitosan films with the aim to provide improved cell adhesion and proliferative properties compared to non-grafted chitosan films. Amidification of the carboxylic acid groups of the peptide onto the amine moieties on the chitosan surface was obtained using EDC-HCl to activate the carboxylic acid functions, with NHS used to create a more stable intermediate.[19] As the NHS reacts with the peptide activated by EDC-HCl, a side product of 3-(((ethyl amino)(hydroxy)methylene)amino)-N,N-dimethylpropan-1-amine (EDH-HCl) is produced (Fig. S-3 in Electronic Supplementary Material).

Separation of reactants and products

The reactants and soluble products of RGDS peptide grafting were monitored using free-solution CE in sodium borate buffer, leading to a strong electro-osmotic flow (EOF, 1.99 to $3.68 \times 10^{-6}$ $m^2 \cdot V^{-1} \cdot s^{-1}$). The pure reactants EDC-HCl, NHS and RGDS were first injected individually (Fig. 1a). Each of the components was fully separated within 4 min and no sample preparation was required (neither for purification nor for derivatization): this fast separation (10 min in total including flushes) allowed real-time monitoring of the grafting

reaction (Fig. 1b and Fig. S-5 in Electronic Supplementary Material) throughout the 18 hour reaction period. The positively charged ammonium group of EDC-HCl resulted in electrophoretic mobility in the same direction as the EOF, thus allowing it to migrate towards the detector the fastest. Conversely, anionic compounds under these conditions, such as NHS and the peptide RGDS had an electrophoretic mobility in the opposite direction to the EOF (due to their hydroxyl and carboxylic acid groups, respectively) leading to a counter-EOF separation and a slower migration (Fig. S-4 in Electronic Supplementary Material). The repeatability and reproducibility of the separation were determined (Table 2), and showed that the precision and accuracy of the electrophoretic mobility were sufficient to prevent any error in peak identification. The UV absorbance of the peptide solution increased linearly with concentration with a correlation coefficient of 0.992 (Fig. S-7a in Electronic Supplementary Material) thus allowing its accurate quantification. The limit of detection (LOD) was 6.0 µM and the limit of quantification (LOQ) was 20.3 µM (Fig. S-7 b in Electronic Supplementary Material), well below the peptide concentration in the grafting mixture that was typically around 500 µM.

Control experiments

The importance of removing acetic acid adsorbed in the chitosan films was demonstrated by failed preliminary grafting experiments (see Electronic Supplementary Material: page 4, as well as characterization by CE, Fig. S-11 and by $^{1}H$ and $^{13}C$ SPE-MAS NMR spectroscopy, Fig. S-14). It is also important to consider leaching of acetic acid from the chitosan films for other applications where chitosan films cast from acetic acid are used such as bioadhesives or for drug delivery. A low (3 %) yield of consumed peptide (and therefore low yield of grafting onto the chitosan films) was attributed to a competing reaction where the acetic acid was grafted onto the films instead of the RGDS. The grafting was thus repeated after rinsing the initial films in PBS. The consumption of peptide was monitored and reached 52-58 % after 4

h, and 60-66 % after 18 h (Fig. 2). This compares well with the 53 % and 83 % grafting determined by HPLC for photochemically grafted GRGD peptide on chitosan.[20] Rinsing the films removed excess acetic acid, and thereby prevented the competing reaction. However, as a result of soaking in PBS the chitosan films swelled. The adsorption (and potentially absorption) of RGDS onto (into) the film could lead to peptide consumption as monitored by CE, a clearly undesirable event as covalent binding of the peptide to the film is required for optimal reproducible cell attachment. To test for adsorption/absorption, control experiments were undertaken without possible grafting or without possible adsorption/absorption by performing sham grafting experiments without the coupling agents (EDC-HCl and NHS) and without the chitosan film (respectively). The control experiment Control-NoCoupling showed peptide adsorbing onto the film (Fig. 3) but in relatively limited amounts, with less than 20 % of peptide consumption compared to 60-66 % in the presence of the coupling agents (see Fig. 2 and corresponding text below). This data demonstrate that at least two thirds of the consumed peptide was covalently grafted onto the chitosan film and not adsorbed. Moreover, when the reaction medium (not the film) was replaced with fresh PBS after 120 min, the fresh PBS monitored 42 min after replacement showed that only about 2 % of the initial peptide was released from the film (Fig. 3). This data indicated that the peptide adsorbed on the film would only be removed by a strong washing procedure.

Another control was performed by replacing the chitosan film with a glucosamine (GLcN) solution (Fig. 2 and 3). The reaction medium with GLcN showed signals with the same electrophoretic mobility as in the case of grafting to the film when monitored by CE, with additional detection of the GLcN coupled to the RGDS peptide at a lower mobility (Fig. S-6). In the GLcN solution the RGDS consumption was about 16 % whereas the peptide consumption in the presence of the film was much greater (even taking into account the adsorption onto the film, which may be up to the amount observed in the absence of the coupling agent). This indicated a higher amount of free -$NH_2$ functional groups on the film

compared to the GLcN solution and also that the amount of available amine (or potentially alcohol group) may be the limiting factor in this grafting experiment. Consequently, the reactant quantities used in this study were adequate for the films and enabled the maximal possible amount of peptide to be covalently grafted onto the films. By scaling the evolution of the peak area of the peptide in the presence of GLcN to the evolution of this peak area in the presence of the film, the ratio of free amine groups between the GlcN and the chitosan film could be determined (Fig. S-10 in Electronic Supplementary Material). This showed that the maximum amount of peptide that could be covalently bound to the chitosan surface of the film was 5,600 RGDS units per nominal $nm^2$ (the nominal surface largely underestimates the effective surface as discussed below). This, however, does not consider that the peptides could also be coupled to one another.

Polycondensation

The last control experiment investigated whether the RGDS polymerized through a polycondensation reaction in the (dilute and typical) conditions used. The RGDS peptide possesses one amine functional group and two different carboxylic acids per molecule, thus it could undergo an ABB' polycondensation. Other possibilities of side reactions include degradation or precipitation. However, the disappearance or lower UV absorbance of the peptide from the reaction medium for Control-NoFilm (Fig. 3) related more to the peptide polycondensation (the peptide bonding leading to polypeptide formation). The polycondensation yielded an oligoelectrolyte or polyelectrolyte, with a nominal charge (at pH 9.2) that increased linearly with the degree of polymerization. The electrophoretic mobility of the oligoelectrolytes very likely increases with the degree of polymerization as observed for DNA (for which the degree of polymerization is often named number of base pairs),[40] oligo(styrene sulfonate) [41] and oligoacrylate [36]. If the polycondensation occurred through only one of the two carboxylic acid moieties in the RGDS then it would form linear oligomers

of RGDS (oligoRGDS). However, if both the –COOH groups were bound to -$NH_2$ of other peptides then hyperbranched oligoRGDS would be formed. The polycondensation of RGDS was therefore analyzed (Fig. 4). The pure RGDS peptide (two carboxylic acid moieties) had an electrophoretic mobility of $2.5 \times 10^{-8}$ $m^2$ $V^{-1}$ $s^{-1}$. After 15 min of reaction, the electrophoretic mobility of the peptide peak decreased by 9 % which could be explained by an RGDS functionalized by NHS. Linear oligomers of RGDS at different degrees of polymerization likely corresponded to the small peaks at 2.8, 3.4 and $3.6 \times 10^{-8}$ $m^2$ $V^{-1}$ $s^{-1}$, and would be consistent with the literature and oligoRGDS respectively bearing 3 charges (dimer), 4 charges (trimer) and 5 charges (tetramer). These peaks represented only a small percentage of the sample. After 15 min, the electrophoretic mobility of the main peptide-related peak decreased to less than half of the original value. The electrophoretic mobility of the main peak (0.3 to $1 \times 10^{-8}$ $m^2$ $V^{-1}$ $s^{-1}$ after 15 min) was too low to correspond to linear oligoRGDS or polyRGDS chains of higher degrees of polymerization. A decrease in electrophoretic mobility can also be caused by branching in the macromolecular structure, as observed for dendrimers [42] and hyperbranched polymers [43]. In addition, the low RGDS concentration did not favor the obtainment of high molecular weights (polymers). The RGDS polycondensation thus likely led to branched oligoRGDS. The electrophoretic mobility of the oligoRGDS peak during the grafting process ($1.1 \times 10^{-9}$ $m^2 \cdot V^{-1} \cdot s^{-1}$, Fig. 2a) was observed to be significantly lower than that of RGDS ($2.4 \times 10^{-9}$ $m^2 \cdot V^{-1} \cdot s^{-1}$, Fig. 4). This polypeptide formation results in some heterogeneity on the surface of the grafted chitosan film since the grafted oligoRGDS have a distribution of molecular weights as well as likely a distribution of branching topologies. Importantly, the formation of the oligoRGDS could increase the accessibility of RGDS to cells should the peptides be grafted in nanometric crevices of the chitosan film.

Peptide quantification

The quantification of the peptide by CE exhibited a good repeatability (Table 2). The grafting as monitored by CE first appeared to be poorly reproducible (see data recorded for Grafted-2h and Grafted-2h-d in Fig. S-8). This was attributed to the polycondensation, evidenced above, continuing during the storage of aliquots of the reaction medium before their analysis by CE. The grafting was therefore monitored in real time with the aliquots injected into the capillary less than 15 min after sampling. The grafting was then observed to be reproducible from film to film, although some small variations were still observed (Fig. 4). Online monitoring of the grafting, as developed for fermentation processes,[44] would lead to an even more accurate monitoring. This is however beyond the scope of this work, for which our offline monitoring was of sufficient accuracy to optimize the grafting process.

The consumption of both EDC-HCl and NHS was also calculated and compared to the peptide consumption (Fig. S-9 in Electronic Supplementary Material) with the EDC-HCl consumption showing a somewhat greater variability compared to the peptide consumption. EDC-HCl consumption also reached a point (at 18 h) where it was not detected anymore. This was potentially due to adsorption of EDC-HCl onto the capillary (due to the positive charge of the capillary and the negative zeta potential of the EDC-HCl) as well as the slow hydrolysis of EDC-HCl in the aqueous medium. By comparison, the concentration of NHS within the reaction mixture was determined with greater precision than that of EDC-HCl. This was expected since the NHS charge is the same as that of the capillary wall, minimizing adsorptive interactions. However, NHS consumption cannot be used to indicate peptide grafting, as NHS is regenerated to its original structure after reaction with RGDS. Together, these data indicate that the RGDS signal was the most appropriate to use for a robust, real-time monitoring of peptide consumption via CE during the grafting experiments.

Reaction monitoring

The amount of peptide used in comparison to the amount of chitosan film used was taken from values obtained from literature [19]. The reaction was continued for at least 18 h, with no significant increase in the amount of grafted peptide observed compared to 4 h of reaction (Fig. 2b). The maximal possible extent of grafting was thus achieved in 4 h in these conditions. Several factors might have influenced the grafting efficiency on different films (Fig. 2b). Assuming that the amount of grafted RGDS equals the amount of RGDS consumed during the CE monitoring, then the 60-66 % yield corresponded to 417-460 RGDS peptide units per nominal $nm^2$. Taking into account the controls data showing RGDS adsorption in the absence of the coupling reagents, the percentage of RGDS calculated as grafted to the surface was reduced to 43-49 % of the initial RGDS. This corresponded to 280-320 RGDS molecules per nominal $nm^2$ or about $5.10^{-8}$ $mol.cm^{-2}$. This is more than one order of magnitude higher than the grafting of $10^{-9}$ $mol.cm^{-2}$ determined by AAA for the grafting of GRGDS through its amine function on modified (carboxylated) chitosan [45]. The discrepancy between the two grafting assessments is likely explained by the different grafting procedures or by an underestimate of the grafting with AAA. The data shown here indicate that the effective surface of the film (including surface roughness) has to be at least two orders of magnitude larger than the nominal one (i.e., the surface of a perfectly smooth film of equivalent dimensions). Note that the fact that oligoRGDS chains of a few RGDS units are grafted rather than individual RGDS peptides only reduces the number of grafted molecules by a small factor, not an order of magnitude. Since the chitosan films were not cast in a controlled environment (e.g., humidity, temperature) they might have exhibited variations in their surface roughness that could have resulted in the films having different actual surface areas for the same nominal surface area (and thus different grafting efficiencies). To examine this, the film surface before grafting was observed via scanning electron microscopy (SEM) (Fig. S-12 in Electronic Supplementary Material). From this data the film surfaces appeared relatively flat and homogeneous on the µm scale (the micrometric indentations and ripples

observed in Fig. S-12b are not present throughout the entire films and are an indication of the film drying process). Higher resolution SEM to better resolve the surface of the films was not possible due to film melting caused by the electron beam (Fig. S-12c). The homogeneous, even and non-porous topography of the films on the μm scale is beneficial as it provides an even surface area for substantial cell adhesion. However, the structure of the films surface may be different at the nanometer scale, which is relevant for the peptide grafting (RGDS only has 4 amino acids, thus RGDS or its oligomers cannot be resolved at the μm scale). Spectroscopy-based techniques were thus used to assess the presence of the peptides on the grafted films.

**Characterization of the films by FT-IR and solid-state NMR**

To complement the indirect measurement of peptide grafting onto the film with a direct measurement, solid-state characterization methods were used. Attenuation Total Reflectance Infrared (ATR IR) analysis was first chosen as it provides a fast and simple spectroscopy method compared to other methods such as solid-state NMR (i.e., ATR IR requires no tedious sample packing and only takes several minutes). The free amine groups and their disappearance through grafting have previously been detected by other groups using IR,[22] while the amide on GRGD peptide has previously also been selectively detected [20]. The ATR IR spectra of chitosan powder and films (Fig. S-13 in Electronic Supplementary Material) were in agreement with those shown in the literature, confirming the molecular structure of the chitosan used [46]. The RGDS grafted onto the chitosan films (expected at 1566 and 1414 $cm^{-1}$ [18]) could not be detected here using ATR IR spectroscopy because of insufficient resolution (overlap of chitosan and peptide signals) or of insufficient sensitivity (due to the limited peptide quantity relative to the chitosan which constitutes the bulk of the films). The free amine group on the chitosan films could not be detected, as shown by comparison with the IR spectrum of glucosamine, and may indicate their involvement in extensive hydrogen bonding.

Due to the limited data obtained through ATR IR solid-state NMR was performed. $^{13}C$ NMR spectra of chitosan Control-soaked film (Fig. S-14 in Electronic Supplementary Material) corresponded to those found in the literature and confirmed the chitosan molecular structure [3, 31]. The $^{13}C$ SPE-MAS NMR spectra of the samples Control-soaked and Grafted-3h (Fig. S-15 in Electronic Supplementary Material) showed no significant difference and therefore no indication of RGDS grafted onto the chitosan film. This may have been due to the low concentration of peptide within the samples. Attempts to increase the films' packing into the rotor by stacking discs of films instead of rolling the films, by altering the contact time and relaxation delays, and by significantly increasing the number of scans were unsuccessful at detecting the peptide's signals. However, swelling the chitosan films with PBS yielded spectra with increased resolution via increased molecular dynamics. Note that sample swelling also introduces a likely heterogeneity of chain dynamics and relaxation behaviors in the samples, rendering any quantification hazardous even with long relaxation delays; for that reason, shorter relaxation delays were chosen to increase sensitivity of the $^{13}C$ NMR experiments. The $^{1}H$ MAS NMR spectrum of Grafted-18h films swollen with PBS revealed two additional peaks, at 1.3 and 4.72 ppm, compared to that of the Control-soaked films swollen with PBS (Fig. 5). The peak at 4.72 ppm was assigned to the α-H of aspartic acid of RGDS (in agreement with the reported value of 4.75 ppm [47]). Although the reported signal assignment of RGDS was sparse and incomplete, a ChemNMR estimation yielded a $^{1}H$ NMR signal for β-H of arginine at 1.55 ppm which is in agreement with the peak observed at 1.3 ppm. ChemNMR estimations yielded a signal at 4.86 ppm corresponding to the α-H of aspartic acid. The slight difference in chemical shift could be accounted for by molecular packing effects experienced in solid-state NMR spectroscopy [48]. The discussion above assumes that the grafting occurred on the amine groups of the chitosan. Estimations by ChemNMR for grafting occurring at the alcohol groups of the chitosan yielded signals at 1.55, 4.86 and 4.62 ppm (Fig. S-17 in Electronic Supplementary Material), where the signal at 4.62

ppm was assigned to the α-H of serine and could also account for the signal observed at 4.72 ppm. However, the signal observed at 4.62 ppm was broad and the assignment could belong to either signal yielded from the ChemNMR estimations, with no significant difference to determine which grafting site was favored. Furthermore, $^{1}$H NMR signals are reported at 0.9 ppm and between 2 - 4 ppm for the coupling agent EDC-HCl [49], at 2.79 and 4.84 ppm for NHS [50]. These signals were either absent or overlapping with the large chitosan signal in the $^{1}$H MAS NMR spectrum of Grafted-18h (Fig. 5a). These data confirm that the coupling reagents were removed from the swollen films during the soakings in PBS and water after grafting.

The $^{13}$C SPE-MAS NMR spectra for the Grafted-18h films swollen with PBS revealed five additional peaks, at 21.2, 30.6, 32.2, 69.4 and 183.2 ppm, compared to Control-soaked films swollen PBS (Fig. 5b). No $^{13}$C NMR spectra of RGDS-grafted chitosan have been reported in the literature. However, the $^{13}$C NMR signals observed after grafting in this study are in agreement with signals reported for RGDS at 24.27, 28.69 and 37.65 ppm (γ-C of arginine, β-C of arginine, and β-C of aspartic acid, respectively) [47]. The expected RGDS signals reported between 50 and 60 ppm were masked by the chitosan signals. The peak observed at 69.4 ppm was absent from both the published $^{13}$C NMR spectra and the ChemNMR estimations for non-grafted RGDS. However, it was present in the ChemNMR estimation of the grafted RGDS – chitosan polymer as the RGDS α-C of serine. This confirms that RGDS peptides were covalently bound to the chitosan through the terminal carboxylic acid function as expected. Grafting at the amine functional group of the chitosan yielded a signal at 61.4 ppm, in agreement with the experimental value of 69.4 ppm. When assuming the grafting of RGDS occurred on the alcohol groups of chitosan, the signal shifted upfield slightly to 62.5 ppm which was in better agreement with the experimental value. Chitosan is expected to yield signals at similar values which were absent from both Grafted-18h and Control-soaked films spectra; this can be explained by the increased dynamics of the α-C compared to the dynamics

of the bulk chitosan film. The ChemNMR estimation produced peaks from 173.2 to 170.3 ppm, corresponding to the various carbonyl α-C when grafted at the amine and the alcohols. A grafting site bias between the amine and the alcohol groups cannot be conclusively determined.

A ChemNMR estimation for NHS and EDC-HCl yielded $^{13}C$ NMR signals at 25.7 and 169 ppm, and 25.2 and 35.4 ppm, respectively, that may correspond to some of the peaks identified as RGDS. However, they do not account for the additional signals obtained in the NMR analysis of Grafted-18h films compared to the Control-soaked film spectra. The $^{13}C$ SPE-MAS NMR spectra (Fig. 5b) cannot reveal if the EDC-HCl and NHS coupling agents were removed from the films, but this can be concluded from the $^{1}H$ MAS NMR (Fig. 5a). Overall, both the $^{13}C$ and $^{1}H$ NMR spectra confirmed that RGDS was successfully covalently grafted onto the chitosan films.

**Cell culture**

To assess whether covalent grafting of the RGDS peptide increased cell attachment to the chitosan film, ARPE-19 and FHL124 cell lines were plated onto non-grafted and grafted films. Both cell lines preferentially attached to the RGDS-grafted chitosan film compared to the non-grafted film (Fig. 6a, 6b). For the ARPE-19 cell line, these cells maintained their morphology, and subsequently proliferated to confluence on the RGDS-grafted chitosan films similar to ARPE-19 cells cultured on tissue culture plastic (Fig. 6a, c). In contrast, the FHL124 cells attached briefly (overnight) to the grafted films but not to the non-grafted films, however, they did not proliferate to confluence and eventually detached from the film. These findings are consistent with the RGDS-grafted chitosan film mimicking fibronectin, and thus being better suited to supporting the retinal ARPE-19 cell line (as fibronectin is a component of Bruch's membrane) [51] but not the lens epithelial FHL124 cell line (as laminin and collagen are the major components of the lens capsule) [52]. It should be noted that some variability in cell attachment was seen between different RGDS-grafted films. This was likely

due to the expected heterogeneity in the chitosan film structure (since the films were cast from a dispersion and not a true solution) which would have then affected the uniform distribution of grafted peptides. It could also be due in part to the attachment of some RGDS peptides to the chitosan through the side chain of aspartate, which contains a carboxylic acid group, rather than through their C-terminal. The formation of longer peptide chains as a result of polycondensation would decrease the number of RGDS-containing molecules grafted onto the film, which in turn could result in incomplete coverage over the film surface.

To determine whether the ARPE-19 cells retained key molecular features after culture on the RGDS-grafted chitosan, messenger RNA (mRNA) expression of the transcription factors *PAX6* and *MITF* was assessed via RT-PCR. These data clearly show that both of these key genes remain expressed after at least 6 days culture on the RGDS-grafted chitosan (Fig. 6d).

## Conclusion

The production of chitosan films grafted with RGDS is not possible by a simple adsorption process. Alternatively, peptides such as RGDS can be covalently grafted onto free-standing chitosan films using the coupling agents EDC-HCl and NHS in one step without prior chitosan modification. The grafting takes place through the carboxylic acid functional group(s) of the peptide and the amine (or alcohol) functional groups on the chitosan surface. This grafting should be monitored in real time and this can be achieved using free-solution CE. CE can separate all reactants and products in only 10 minutes and it requires no sample preparation: it is thus an ideal indirect technique for real-time monitoring of the grafting process. The data presented here revealed that adsorption of RGDS peptide on the chitosan film takes place but is not the main method of RGDS attachment to the chitosan. While covalent grafting had been considered as a “more involved process” than adsorption [11], it was shown in the present work that grafting directly on the amine of the chitosan allows for a simple covalent grafting method. Side reactions of the RGDS peptide, such as

polycondensation, are significant in the absence of chitosan film and it is thus important to monitor the grafting in real time to obtain accurate results. The $^{1}H$ and $^{13}C$ NMR spectroscopy of the swollen films directly demonstrated the covalent grafting of RGDS onto the film. All available free amine (alcohol) functional groups on the chitosan film surface had reacted, leading to a high density of RGDS on the surface. The RGDS was present in the form of (likely branched) oligomers of RGDS. The SEM data indicated the RGDS-grafted films had a flat surface on the micrometer (cell) scale, but nanometric-scale crevices likely exist [53]. Given the approximate 5-10 μm diameter of the ARPE-19 and FHL124 cells used here, these nanometer-scale crevices would be inaccessible for cell attachment. Considering the order of magnitude difference between the size of a cell and the size of the RGDS, the formation of oligoRGDS might help bring a higher number of RGDS moieties in contact with the cells, rather than being inaccessible in nanometric crevices. However, the surface of the films may also present some chemical heterogeneity with zones richer in acetyl groups, thus poorer in free amine groups on which RGDS grafting occurs. This could account for some of the inter-film cell attachment variability seen.

Further development of chitosan films could be undertaken by casting them from solutions or other dispersions, in order to circumvent potential differences in surface roughness and surface chemical heterogeneity between films and thereby produce films with a more homogeneous/accessible peptide grafting surface for cell attachment. Film preparation prior to grafting could also be completed to deacetylate the surface of the films; this could increase the number of active sites available for peptide attachment in order to further decrease variability in cell attachment. The use of isotopically labeled peptides would increase the sensitivity for the detection and quantification of peptide grafting through NMR spectroscopy. Further studies of the chitosan film itself could be carried out by 13C and $^{15}N$ MAS NMR spectroscopy. [3] While both ARPE-19 and FHL124 are ocular cell lines, they are derived from different tissues that require different extracellular matrix interactions. This was

supported by the ability of the ARPE-19 cells, but not the FHL124 cells, to attach and proliferate on the RGDS-grafted chitosan. Thus the above CE-based method will enable future chitosan films to be optimized for attachment by particular cell types, through the ability to monitor in real time the attachment of different extracellular matrix peptide mimetics. Importantly, these peptide mimetics can be chosen based on the in vivo extracellular matrix requirements for the particular cell type(s) of interest.

## Acknowledgements

CL, MO'C and MG thank the University of Western Sydney for an International Research Initiatives Scheme (IRIS) grant. Mariam Mnatsakanyan (UWS) is thanked for the production of some of the chitosan films. We would like to acknowledge the Advanced Materials Characterisation Facility (AMCF) of UWS for assistance and access to the instrumentation.

## Conflict of interest

The authors declare that they have no conflict of interest.

## References

1. Dash M, Chiellini F, Ottenbrite RM, Chiellini E (2011) Chitosan-A versatile semi-synthetic polymer in biomedical applications. Prog. Polym. Sci. 36:981-1014
2. Domard A (2011) A perspective on 30 years research on chitin and chitosan. Carbohydr. Polym. 84:696-703
3. Gartner C, Lopez BL, Sierra L, Graf R, Spiess HW, Gaborieau M (2011) Interplay between Structure and Dynamics in Chitosan Films Investigated with Solid-State NMR, Dynamic Mechanical Analysis, and X-ray Diffraction. Biomacromolecules 12:1380-1386
4. Rinaudo M (2006) Chitin and chitosan: Properties and applications. Prog. Polym. Sci. 31:603-632
5. Martínez-Camacho AP, Cortez-Rocha MO, Ezquerra-Brauer JM, Graciano-Verdugo AZ, Rodriguez-Félix F, Castillo-Ortega MM, Yépiz-Gómez MS, Plascencia-Jatomea M (2010) Chitosan composite films: Thermal, structural, mechanical and antifungal properties. Carbohydr. Polym. 82:305-315
6. Shi CM, Zhu Y, Ran XZ, Wang M, Su YP, Cheng TM (2006) Therapeutic potential of chitosan and its derivatives in regenerative medicine. J. Surg. Res. 133:185-192

7. Bodnar M, Hartmann JF, Borbely J (2005) Preparation and characterization of chitosan-based nanoparticles. Biomacromolecules 6:2521-2527
8. Wise JK, Alford A, Goldstein S, Stegemann JP (2014) Comparison of Uncultured Marrow Mononuclear Cells and Culture-Expanded Mesenchymal Stem Cells in 3D Collagen-Chitosan Microbeads for Orthopaedic Tissue Engineering. Tissue Eng. Part A 20:210-224
9. de la Mata A, Nieto-Miguel T, López-Paniagua M, Galindo S, Aguilar MR, García-Fernández L, Gonzalo S, Vázquez B, Román JS, Corrales RM, Calonge M (2013) Chitosan-gelatin biopolymers as carrier substrata for limbal epithelial stem cells. J. Mater. Sci. Mater. Med. 24:2819-2829
10. Chien Y, Liao YW, Liu DM, Lin HL, Chen SJ, Chen HL, Peng CH, Liang CM, Mou CY, Chiou SH (2012) Corneal repair by human corneal keratocyte-reprogrammed iPSCs and amphiphatic carboxymethyl-hexanoyl chitosan hydrogel. Biomaterials 33:8003-8016
11. Jiang T, Kumbar SG, Nair LS, Laurencin CT (2008) Biologically active chitosan systems for tissue engineering and regenerative medicine. Curr. Top. Med. Chem. 8:354-364
12. Li Z, Leung M, Hopper R, Ellenbogen R, Zhang M (2010) Feeder-free self-renewal of human embryonic stem cells in 3D porous natural polymer scaffolds. Biomaterials 31:404-412
13. Shekaran A, Garcia AJ (2011) Nanoscale engineering of extracellular matrix-mimetic bioadhesive surfaces and implants for tissue engineering. Biochim. Biophys. Acta Gen. Subj. 1810:350-360
14. Gristina A (1987) Biomaterial-centered infection: microbial adhesion versus tissue integration. Science 237:1588-1595
15. Boateng SY, Lateef SS, Mosley W, Hartman TJ, Hanley L, Russell B (2005) RGD and YIGSR synthetic peptides facilitate cellular adhesion identical to that of laminin and fibronectin but alter the physiology of neonatal cardiac myocytes. Am. J. Physiol. Cell Physiol. 288:C30-38
16. Smith E, Yang J, McGann L, Sebald W, Uludag H (2005) RGD-grafted thermoreversible polymers to facilitate attachment of BMP-2 responsive C2C12 cells. Biomaterials 26:7329-7338
17. Custodio CA, Alves CM, Reis RL, Mano JF (2010) Immobilization of fibronectin in chitosan substrates improves cell adhesion and proliferation. J. Tissue Eng. Regen. Med. 4:316-323
18. Karakecili AG, Gumusderelioglu M (2008) Physico-chemical and thermodynamic aspects of fibroblastic attachment on RGDS-modified chitosan membranes. Coll. Surf. B Biointerf. 61:216-223
19. Cheng N, Cao XD (2011) Photosensitive chitosan to control cell attachment. J. Coll. Interf. Sci. 361:71-78
20. Chung TW, Lu YF, Wang SS, Lin YS, Chu SH (2002) Growth of human endothelial cells on photochemically grafted Gly-Arg-Gly-Asp (GRGD) chitosans. Biomaterials 23:4803-4809
21. Han HD, Mangala LS, Lee JW, Shahzad MMK, Kim HS, Shen D, Nam EJ, Mora EM, Stone RL, Lu C, Lee SJ, Roh JW, Nick AM, Lopez-Berestein G, Sood AK (2010) Targeted Gene Silencing Using RGD-Labeled Chitosan Nanoparticles. Clin. Cancer Res. 16:3910-3922
22. Ho MH, Wang DM, Hsieh HJ, Liu HC, Hsien TY, Lai JY, Hou LT (2005) Preparation and characterization of RGD-immobilized chitosan scaffolds. Biomaterials 26:3197-3206

23. Hansson A, Hashom N, Falson F, Rousselle P, Jordan O, Borchard G (2012) In vitro evaluation of an RGD-functionalized chitosan derivative for enhanced cell adhesion. Carbohydr. Polym. 90:1494-1500
24. Shi ZL, Neoh KG, Kang ET, Poh C, Wang W (2008) Bacterial adhesion and osteoblast function on titanium with surface-grafted chitosan and immobilized RGD peptide. J. Biomed. Mater. Res. Part A 86A:865-872
25. Kašička V (2012) Recent developments in CE and CEC of peptides (2009–2011). Electrophoresis 33:48-73
26. Bao JJ (2000) Separation of proteins by capillary electrophoresis using an epoxy based hydrophilic coating. J. Liq. Chromatogr. Rel. Technol. 23:61-78
27. Geiger M, Hogerton AL, Bowser MT (2011) Capillary Electrophoresis. Anal. Chem. 84:577-596
28. Oliver JD, Gaborieau M, Hilder EF, Castignolles P (2013) Simple and robust determination of monosaccharides in plant fibers in complex mixtures by capillary electrophoresis and high performance liquid chromatography. J. Chromatogr. A 1291:179-186
29. Thevarajah JJ, Gaborieau M, Castignolles P (2014) Separation and characterization of synthetic polyelectrolytes and polysaccharides with capillary electrophoresis. Adv. Chem. 2014:Article ID 798503
30. Mnatsakanyan M, Thevarajah JJ, Roi RS, Lauto A, Gaborieau M, Castignolles P (2013) Separation of chitosan by degree of acetylation using simple free solution capillary electrophoresis. Anal. Bioanal. Chem. 405:6873-6877
31. Heux L, Brugnerotto J, Desbrieres J, Versali MF, Rinaudo M (2000) Solid state NMR for determination of degree of acetylation of chitin and chitosan. Biomacromolecules 1:746-751
32. Lefay C, Guillaneuf Y, Moreira G, Thevarajah JJ, Castignolles P, Ziarelli F, Bloch E, Major M, Charles L, Gaborieau M, Bertin D, Gigmes D (2013) Heterogeneous modification of chitosan via nitroxide-mediated polymerization. Polym. Chem. 4:322-328
33. Lee E, MacLaren RE (2011) Sources of retinal pigment epithelium (RPE) for replacement therapy. Br. J. Ophthalmol. 95:445-449
34. Priglinger SG, Alge CS, Neubauer AS, Kristin N, Hirneiss C, Eibl K, Kampik A, Welge-Lussen U (2004) TGF-beta 2-induced cell surface tissue transglutaminase increases adhesion and migration of RPE cells on fibronectin through the gelatin-binding domain. Invest. Ophthalmol. Vis. Sci. 45:955-963
35. Olivero DK, Furcht LT (1993) Type-IV collagen, laminin, and fibronectin promote the adhesion and migration of rabbit lens epithelial-cells in-vitro. Invest. Ophthalmol. Vis. Sci. 34:2825-2834
36. Gaborieau M, Causon TJ, Guillaneuf Y, Hilder EF, Castignolles P (2010) Molecular weight and tacticty of oligoacrylates by capillary electrophoresis - mass spectrometry. Aus. J. Chem. 63:1219-1226
37. Morcombe CR, Zilm KW (2003) Chemical shift referencing in MAS solid state NMR. J. Magn. Reson. 162:479-486
38. Ungrin M, O'Connor M, Eaves C, Zandstra PW (2007) Phenotypic analysis of human embryonic stem cells. Curr Protoc Stem Cell Biol. 1B.3:1-25
39. O'Connor MD, Wederell E, Robertson G, Delaney A, Morozova O, Poon SSS, Yap D, Fee J, Zhao YJ, McDonald H, Zeng T, Hirst M, Marra MA, Aparicio S, Eaves CJ (2011) Retinoblastoma-binding proteins 4 and 9 are important for human pluripotent stem cell maintenance. Exp. Hematol. 39:866-879
40. Stellwagen NC, Gelfi C, Righetti PG (1997) The free solution mobility of DNA. Biopolymers 42:687-703

41. Cottet H, Gareil P, Theodoly O, Williams CE (2000) A semi-empirical approach to the modeling of the electrophoretic mobility in free solution: Application to polystyrenesulfonates of various sulfonation rates. Electrophoresis 21:3529-3540
42. Ibrahim A, Koval D, Kasicka V, Faye C, Cottet H (2013) Effective Charge Determination of Dendrigraft Poly-L-lysine by Capillary Isotachophoresis. Macromolecules 46:533-540
43. Maniego AR, Ang D, Guillaneuf Y, Lefay C, Gigmes D, Aldrich-Wright JR, Gaborieau M, Castignolles P (2013) Separation of poly(acrylic acid) salts according to topology using capillary electrophoresis in the critical conditions. Anal. Bioanal. Chem. 405:9009-9020
44. Turkia H, Holmström S, Paasikallio T, Sirén H, Penttilä M, Pitkänen J-P (2013) Online Capillary Electrophoresis for Monitoring Carboxylic Acid Production by Yeast during Bioreactor Cultivations. Anal. Chem. 85:9705-9712
45. Li J, Yun H, Gong YD, Zhao NM, Zhang XF (2006) Investigation of MC3T3-E1 cell behavior on the surface of GRGDS-coupled chitosan. Biomacromolecules 7:1112-1123
46. Silva SML, Braga CRC, Fook MVL, Raposo CMO, Carvalho LH, Canedo EL (2012) Application of Infrared Spectroscopy to Analysis of Chitosan/Clay Nanocomposites. In: T. Theophile, (Ed.), Materials Science, Engineering and Technology, InTech, Rijeka.
47. Mickos H, Bahr J, Lüning B (1990) The three-dimensional structure of the RGD (Arg-Gly-Asp) adhesion sequence of fibronectin; NMR studies of the peptides RGDS and GRGDSP. Acta Chem. Scand. 44:161-164
48. Schmidt-Rohr K, Spiess HW (1994) Multidimensional solid-state NMR and polymers. Academic Press Ltd, San Diego, USA
49. Castillo JJ, Torres MH, Molina DR, Castillo-León J, Svendsen WE, Escobar P, Martínez O F (2012) Monitoring the functionalization of single-walled carbon nanotubes with chitosan and folic acid by two-dimensional diffusion-ordered NMR spectroscopy. Carbon 50:2691-2697
50. Spectral database for organic compounds SDBS (2014) National Institute of Advanced Industrial Science and Technology, AIST, Japan. http://sdbs.db.aist.go.jp/sdbs/cgi-bin/cre_index.cgi
51. Das A, Frank RN, Zhang NL, Turczyn TJ (1990) Ultrastructural-localization of extracellular-matrix components in human retinal-vessels and Bruch's membrane. Arch. Ophthalmol. 108:421-429
52. Wederell ED, de Iongh RU (2006) Extracellular matrix and integrin signaling in lens development and cataract. Semin. Cell Dev. Biol. 17:759-776
53. Inthanon K, Saranwong N, Wongkham W, Wanichapichart P, Prakrajang K, Suwannakachorn D, Yu LD (2013) PIII-induced enhancement and inhibition of human cell attachment on chitosan membranes. Surf. Coat. Technol. 229:112-119

**Table 1** Chitosan Samples (films were 10 $cm^2$ films unless otherwise stated).

| Sample | Description |
|---|---|
| Powder | Chitosan powder – used as received |
| Non-treated | Films, untreated |
| Control-soaked | Films gently shaken for 2 h in 10 mL PBS |
| Neutralized | Films immersed in 1 vol% NaOH aqueous solution, then washed thoroughly with MilliQ water. |
| Ethanol-washed | Films gently shaken for 2 h in 10 mL PBS, then washed with 0.1 M ethanol in MilliQ water, fresh PBS and MilliQ water. |
| Grafted-2h, Grafted-2h-d (duplicates) | Films gently shaken for 2 h in 10 mL PBS, then immersed in 10 mL reaction medium containing RGDS, NHS and EDC-HCl for up to 2 h, then washed with fresh PBS and MilliQ water. |
| Grafted-3h, Grafted-3h-d (duplicates) | Films gently shaken for 2 h in 10 mL PBS, then immersed in 5 mL reaction medium containing RGDS, NHS and EDC-HCl for 3 h covered with Parafilm, then washed with fresh PBS and MilliQ water (9 and 8 $cm^2$ films, respectively). |
| Grafted-18h, Grafted-18h-d (duplicates), Grafted-18h-r1 and Grafted-18h-r2 (replicates) | Films gently shaken for 2 h in 10mL PBS, then immersed in 5 mL reaction medium containing RGDS, NHS and EDC-HCl for up to 18 h covered with Parafilm, then washed with fresh PBS and MilliQ water. |
| Control-GLcN | 10 mL of GLcN solution mixed with 2.5 mL reaction medium containing RGDS, NHS and EDC HCl. Solution then gently shaken for 2 h covered with Parafilm. |
| Control-NoCoupling | Films soaked in PBS for 2 h, then immersed in 5 mL PBS containing RGDS only (no EDC-HCl or NHS) for 4 h covered with Parafilm. |
| Control-NoFilm | 5 mL reaction medium containing RGDS, NHS and EDC-HCl for 4 h, but no chitosan film |

**Table 2** Repeatability and reproducibility of the electrophoretic mobilities of reactants and products. Repeatabilities for different operators are separated by a slash (n=8 for operator 1, n=15 for operator 2).

| Compound | Repeatability RSD (%) | Reproducibility RSD (%) |
|---|---|---|
| EDC-HCl | 6.97 / 3.10 | 5.03 |
| EDH-HCl | 5.61 / 3.91 | 4.76 |
| PBS | 12.6 / 3.89 | 8.25 |
| RGDS | 9.85 / 2.92 | 6.39 |
| NHS | 15.5 / 1.90 | 8.70 |

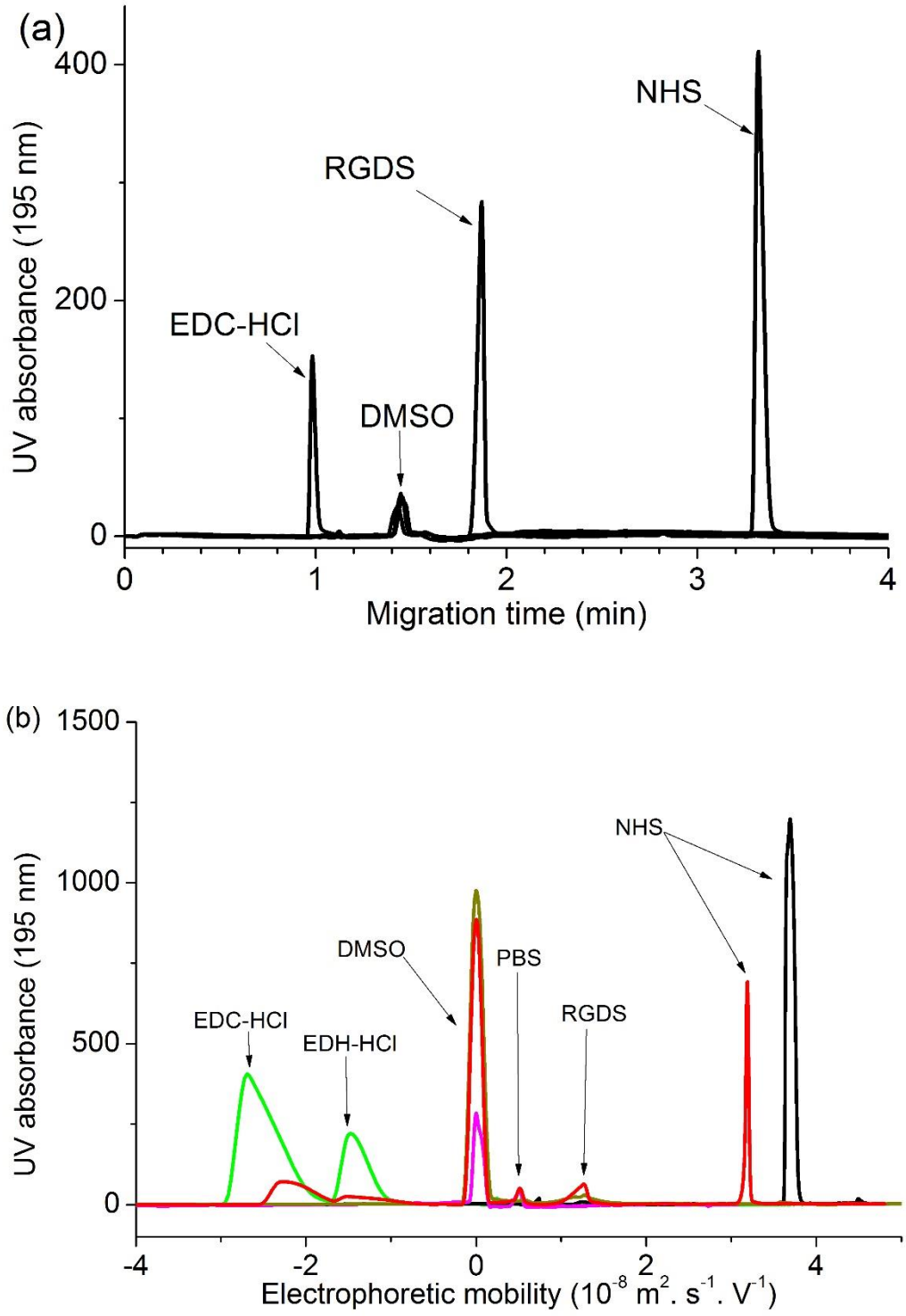


**Fig. 1** Monitoring of the grafting by free-solution CE: (a) separation of reactants, injected individually, as a function of migration time, and (b) electrophoretic mobility distribution of the reaction medium after 15 min reaction (red) and of the individual reactants (other colors)

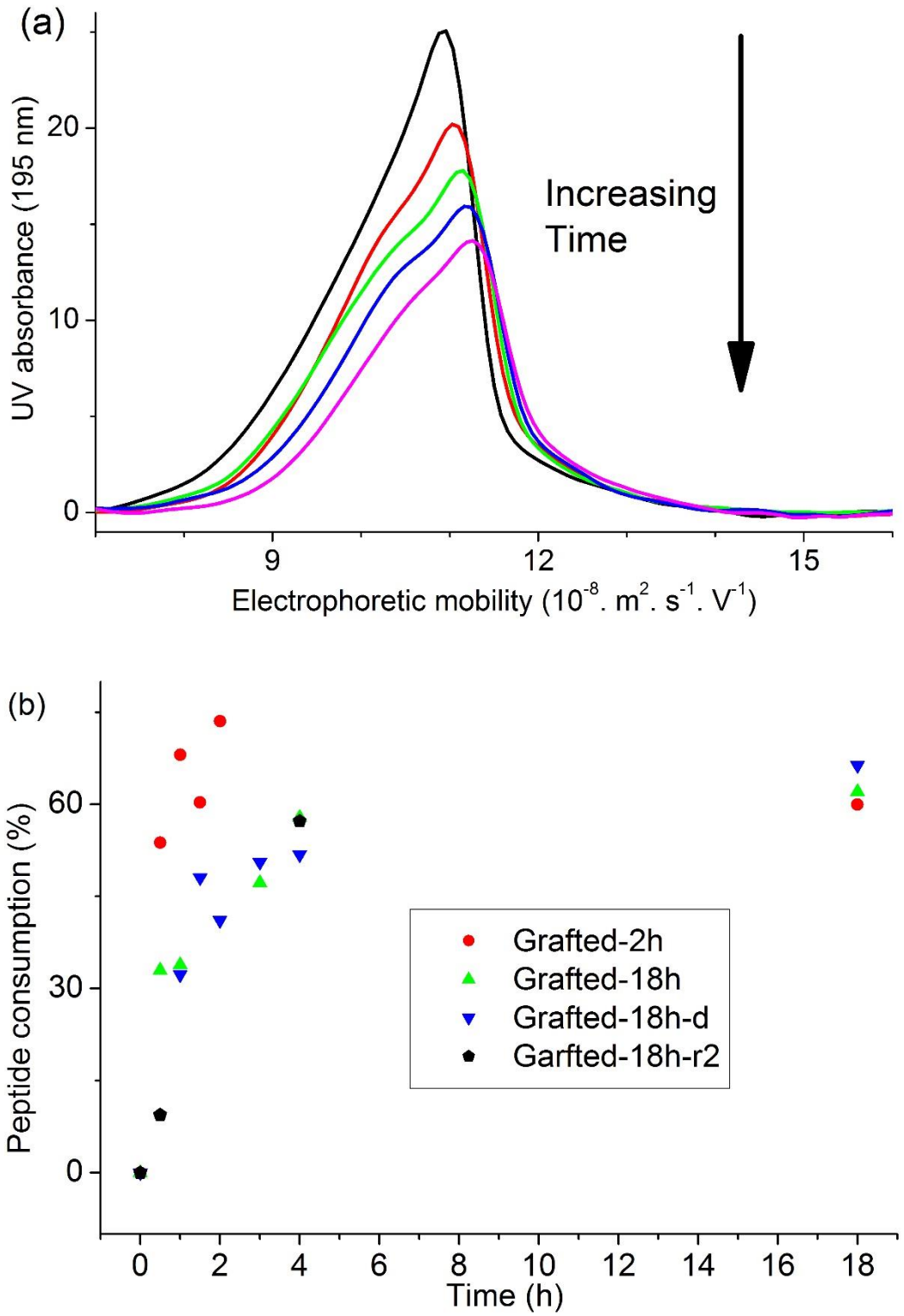


**Fig. 2** a) Electropherograms of RGDS signal showing its consumption over the reaction time in real time (curves are shown for 30, 60, 90, 120, and 150 min reaction times, full electropherograms are on Fig. S-5) b) Real-time monitoring of RGDS peptide consumption during the grafting onto chitosan films with CE (different symbols refer to different grafting reactions, see Table 1)

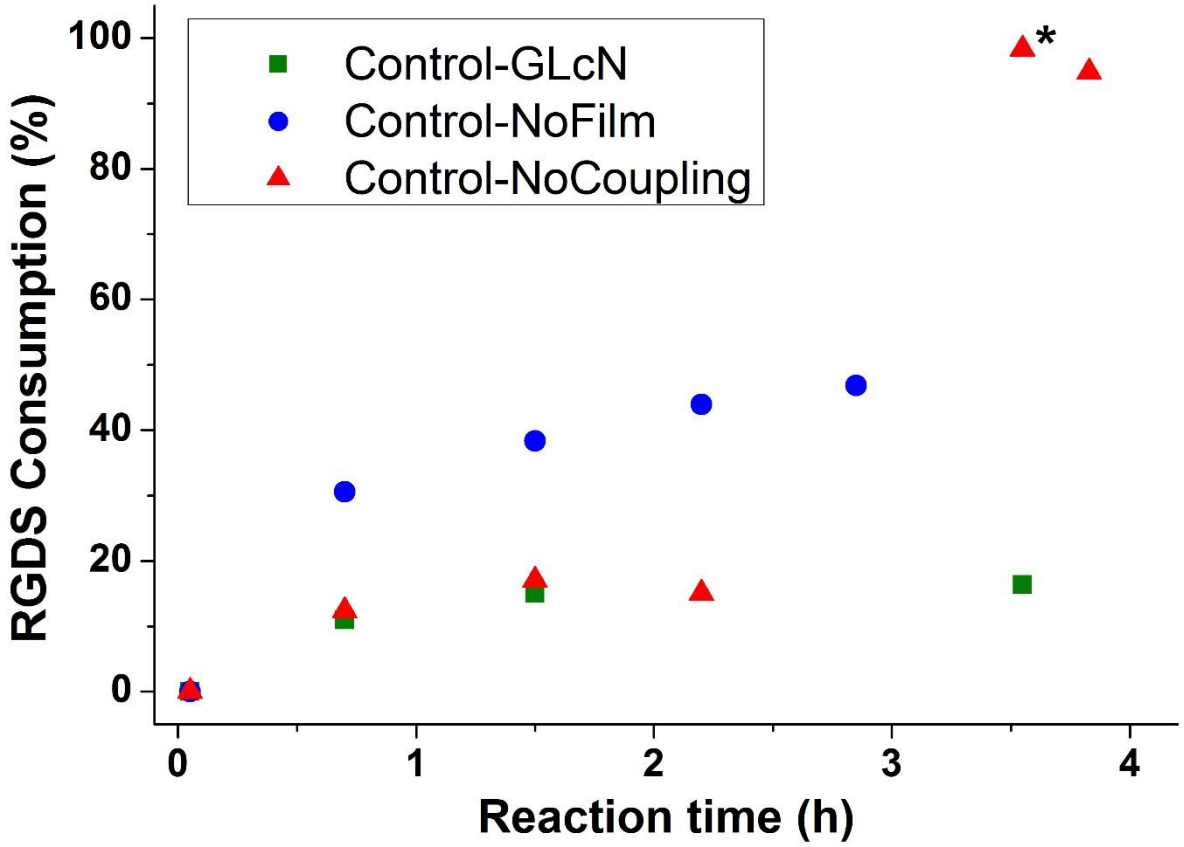


**Fig. 3** RGDS consumption monitored in real time by free-solution CE in control experiments: GLcN solution (Control-GLcN, see electropherograms on Fig. S-6), RGDS with coupling agent (Control-NoFilm) and RGDS without coupling agent showing peptide adsorption (Control-NoCoupling) (Table 1). * indicates that the reaction medium (not the film) was replaced with fresh PBS: the high peptide consumption then was not an indication of grafting or adsorption on the film but simply an indication that all peptide was removed by taking away the reaction medium, and little peptide was released from the film into the fresh PBS

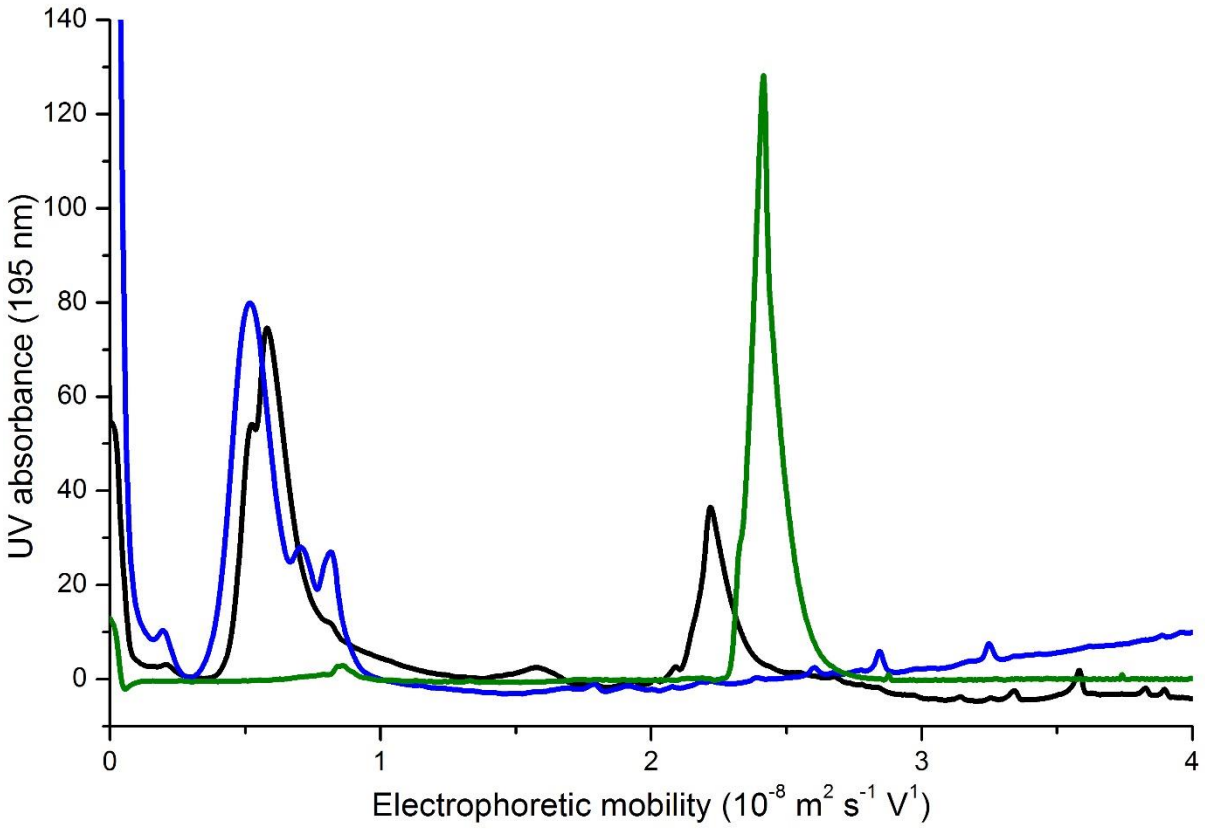


**Fig. 4** Electropherograms of pure RGDS (green) and of the reaction medium initially containing RGDS, EDC-HCl and NHS, also containing oligo/polyRGDS after 15 min (black) and 75 min (blue) reaction

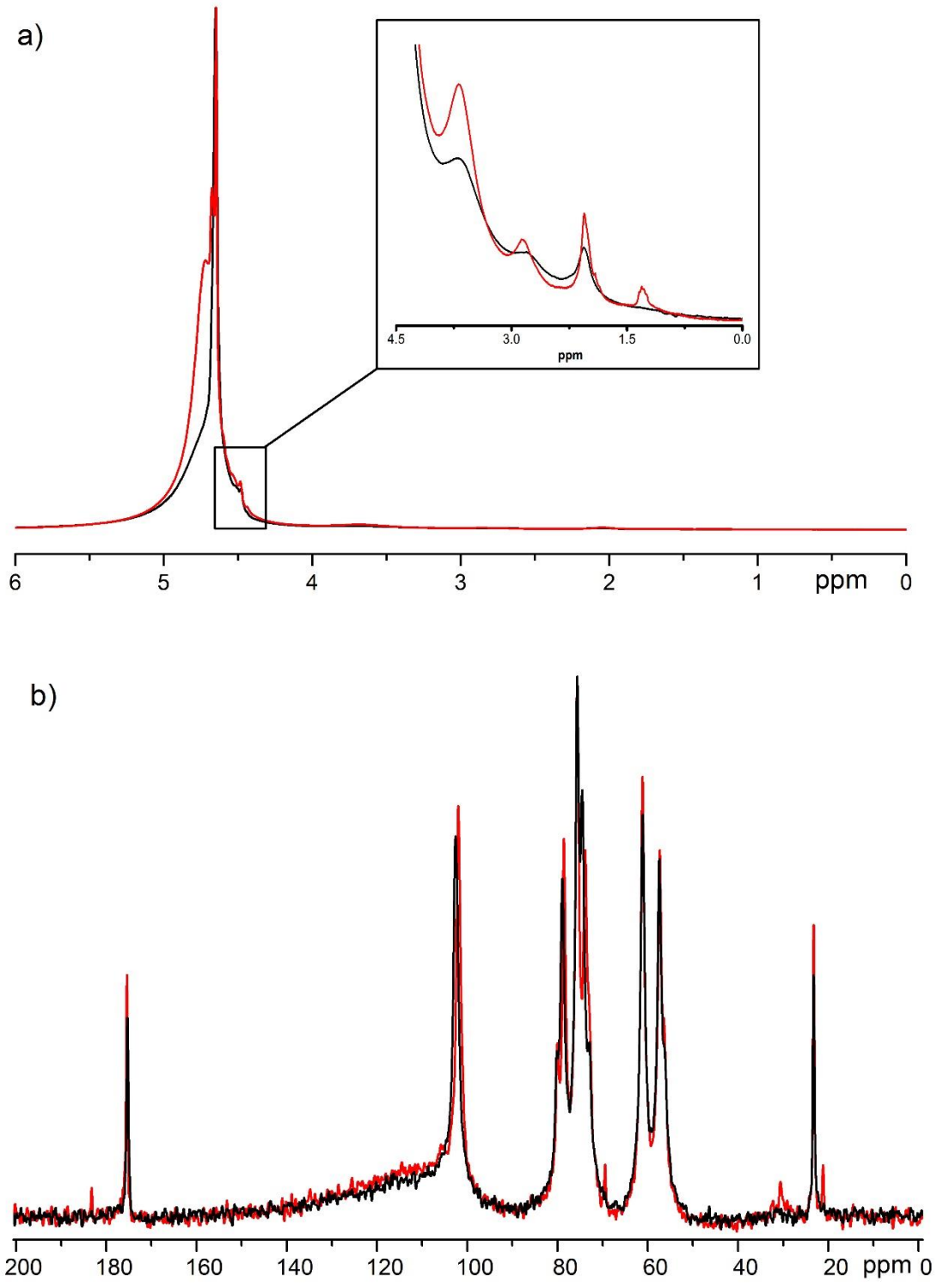


**Fig. 5** NMR spectra of Grafted-18h (red line) and Control-soaked (black line) films swollen with PBS: a) $^{1}H$ MAS NMR spectra, with insert showing a magnification of spectra between 0 and 4.5 ppm, and b) $^{13}C$-SPE MAS NMR spectra

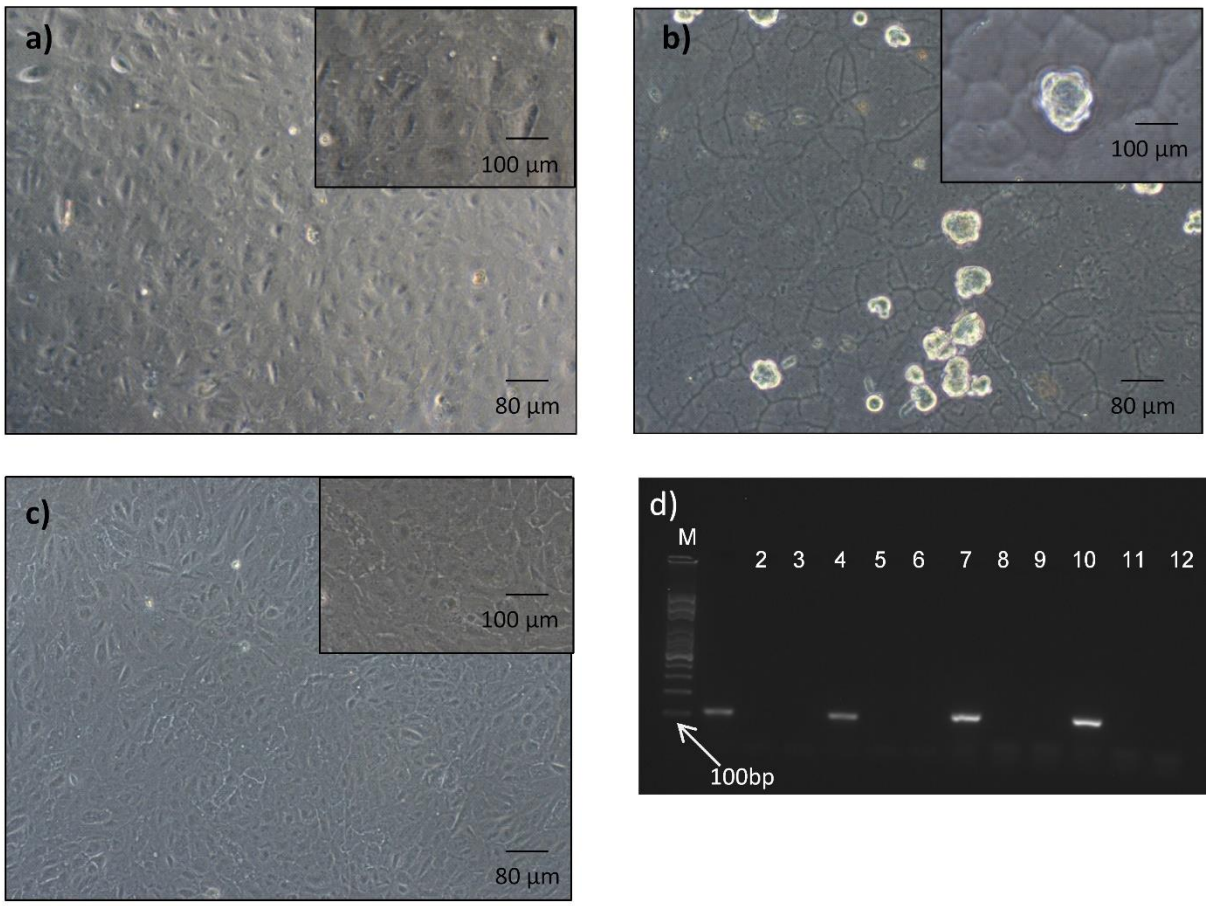


**Fig. 6** Phenotypic characterization of chitosan-cultured cells. a) ARPE-19 cells attached and proliferated to confluence on RGDS-grafted chitosan films. b) ARPE-19 did not attach to the non-grafted chitosan. c) Control ARPE-19 cells plated onto tissue culture plastic (a-c: images shown were taken 7 days after cell seeding, and the inserts show a higher magnification). d) Separated PCR products via agarose gel electrophoresis showing expression of control ARPE-19 cells cultured on plastic for 6 days for *PAX6* (lane 1) and *MITF* (lane 7), and cultured for 6 days on RGDS-grafted films for *PAX6* and *MITF* (lanes 4 and 10, respectively). All amplicons were of the expected size as shown by comparison with the nucleotide marker (M). The control PCR reactions (shown in lanes 2, 3, 5, 6, 8, 9, 11 and 12) indicate that the detected *PAX6* and *MITF* amplicons did not arise from contaminating genomic DNA or DNA-contaminated reagents

**Online abstract figure**

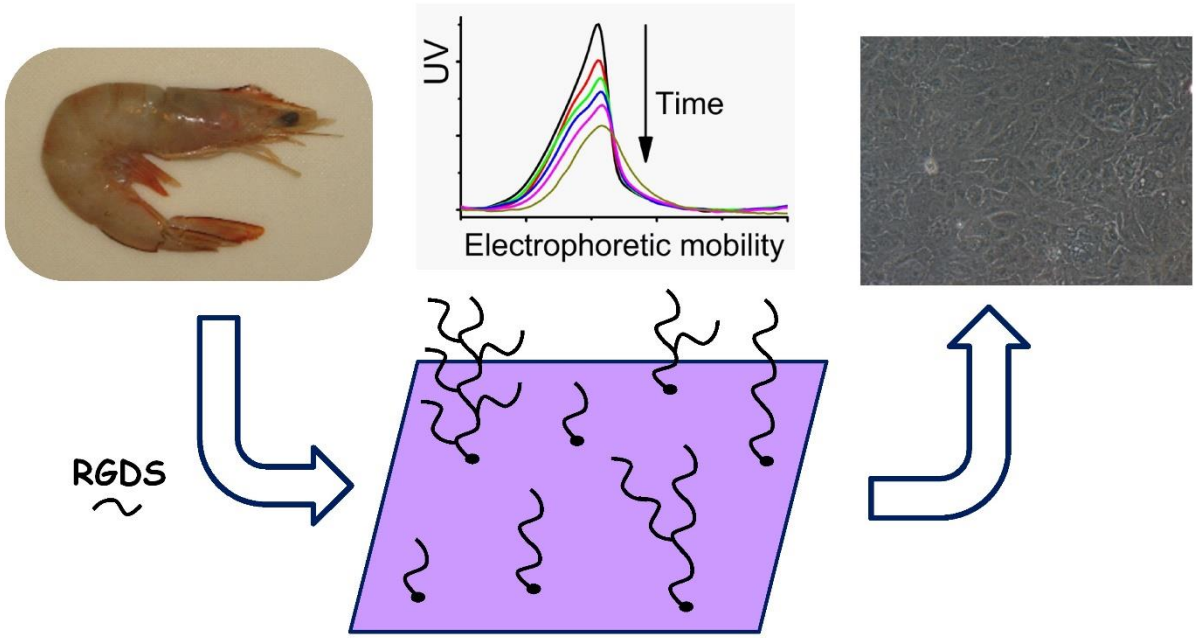

Electronic Supplementary Material for

*Analytical and Bioanalytical Chemistry*

# Real-time monitoring of peptide grafting onto chitosan films using capillary electrophoresis

Danielle L. Taylor[#],[1,2] Joel J. Thevarajah[#],[1,2] Diksha K. Narayan,[1,2,3] Patricia Murphy,[1,3] Melissa M. Mangala,[1,3] Seakcheng Lim,[1,3] Richard Wuhrer,[4] Catherine Lefay,[5] Michael D. O'Connor*,[1,3] Marianne Gaborieau*,[1,2] Patrice Castignolles[2]

1 University of Western Sydney, Molecular Medicine Research Group, Parramatta 2150 / Campbelltown 2560, Australia

2 University of Western Sydney, Australian Centre for Research on Separation Sciences (ACROSS), School of Science and Health, Parramatta 2150, Australia

3 University of Western Sydney, School of Medicine, Campbelltown 2560, Australia

4 University of Western Sydney, Advanced Materials Characterisation Facility (AMCF), Parramatta 2150, Australia

5 Aix-Marseille Université, CNRS, ICR UMR 7273, 13397 Marseille, France

[#]Joel Thevarajah and Danielle Taylor contributed equally

* corresponding authors: (M. O'Connor) e-mail m.oconnor@uws.edu.au, tel +61 2 4620 3902, fax +61 2 4620 3890; (M. Gaborieau) e-mail m.gaborieau@uws.edu.au, tel +61 2 9685 9905, fax +61 2 9685 9905

**Chitosan structure and grafting onto chitosan films**

The structure of the polysaccharide chitosan includes varying proportions of D-glucosamine and *N*-acetyl-D-glucosamine (Fig. S-1). A photograph of a chitosan film cast form acetic acid solution is shown on Fig. S-2. The reaction scheme is shown on Fig. S-3.

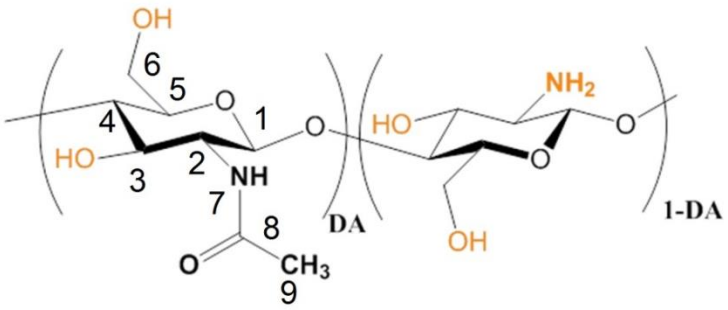


**Fig. S-1** Chemical structure of chitosan with a degree of acetylation DA. Chitin corresponds to DA=1

**Fig. S-2** Photograph of chitosan film cast from aqueous acetic acid

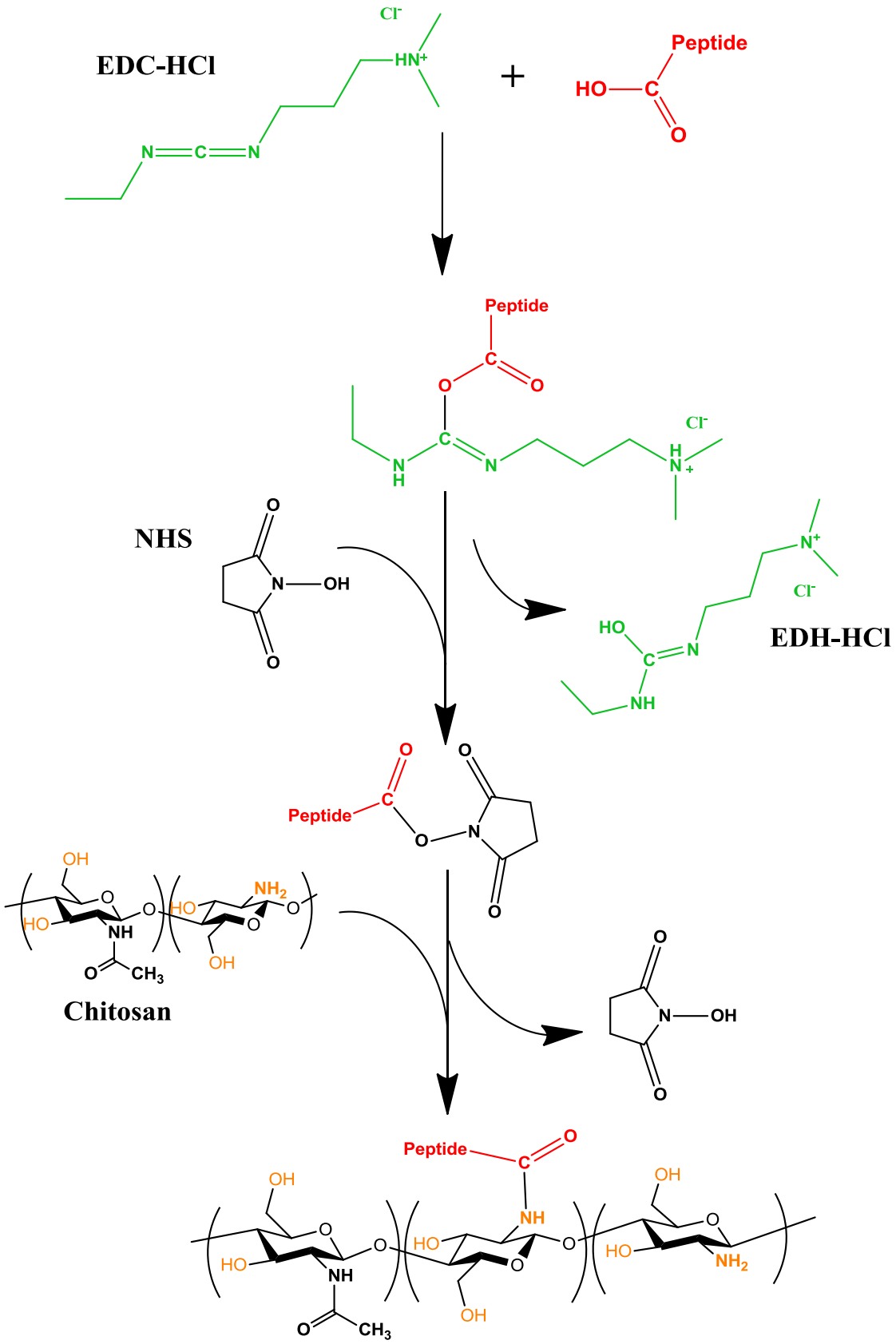


**Fig. S-3** Reaction scheme for peptide grafting onto chitosan film. Note: activated peptide may react with either an amine or an alcohol group of chitosan

Preliminary grafting experiments indicated that only 3 % of peptide was consumed after 2 h. These films were observed to kill cells in less than 24 h (data not shown) if not thoroughly rinsed with PBS indicating either the residual presence of reactant (EDC-HCl is cytotoxic) [1] or the release of acetic acid (as the chitosan films had been cast from suspensions in aqueous acetic acid). Acetic acid was proved to be the cause of the low grafting yield and of the cells death through its identification with capillary electrophoresis (see Fig. S-11) as well as $^{1}H$ and $^{13}C$ SPE-MAS NMR spectroscopy (Fig. S-14) as follows. A non-neutralized chitosan film was placed in MilliQ water: a decrease in pH from 6.00 to 5.36 was observed consistent with the release of acetic acid. This solution in which the film had been immersed was further analyzed via CE, which confirmed that the released molecule had the same electrophoretic mobility as acetic acid (see Fig. S-11 in supporting information). Finally, $^{1}H$ and $^{13}C$ SPE-MAS NMR spectroscopy showed that the film contained acetic acid that was eliminated upon rinsing with PBS for 2 h (Fig. S-14).

**Capillary electrophoresis**

The principle of free solution capillary electrophoresis at high pH in fused silica capillaries is given in Fig. S-4, followed by a calibration curve for the RGDS quantification (Fig. S-7). Fig. S-8 show the results of monitoring the grafting not in real time (defined here as injecting the reaction medium more than 15 min after the aliquot was withdrawn). The consumption of peptide is compared to the one of the coupling agents on Fig. S-9. Fig. S-11 shows the electropherogram of solutions used to rinse the chitosan films, and the comparison with acetic acid solution.

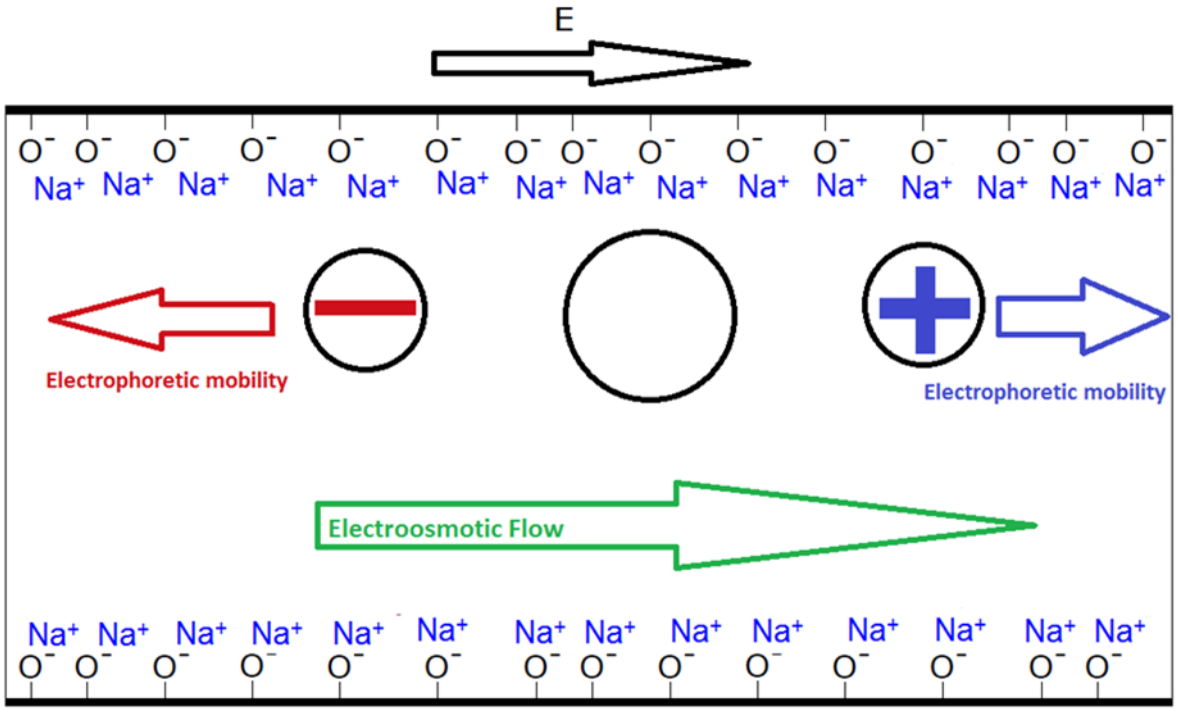


**Fig. S-4** Principle of the separation of compounds by their charge-to-friction ratio under basic conditions (sodium borate, pH 9.2) and a positive voltage (30 kV)

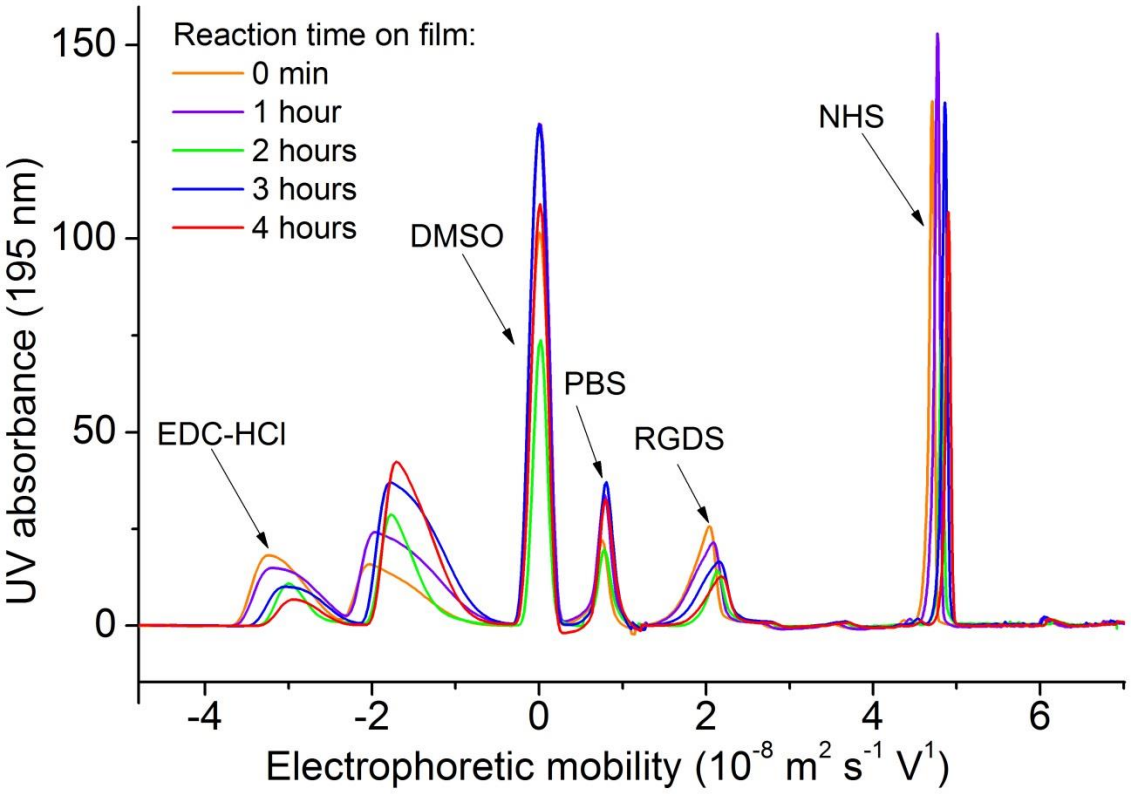


**Fig. S-5** Electropherograms of peptide in the reaction medium in real-time

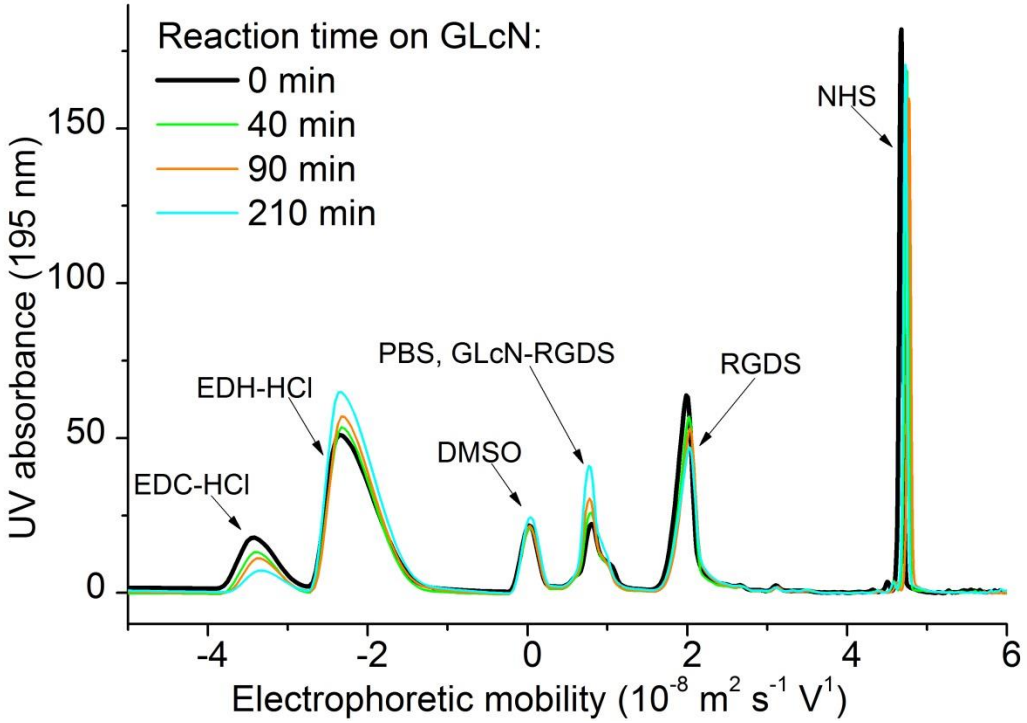


**Fig. S-6** Electropherograms of GLcN solution in the reaction medium in real-time. The shoulder on the right side of the PBS signal at $2.10^{-8}$ $m^2s^{-1}V^{-1}$ is the signal of the GLcN grafted with RGDS

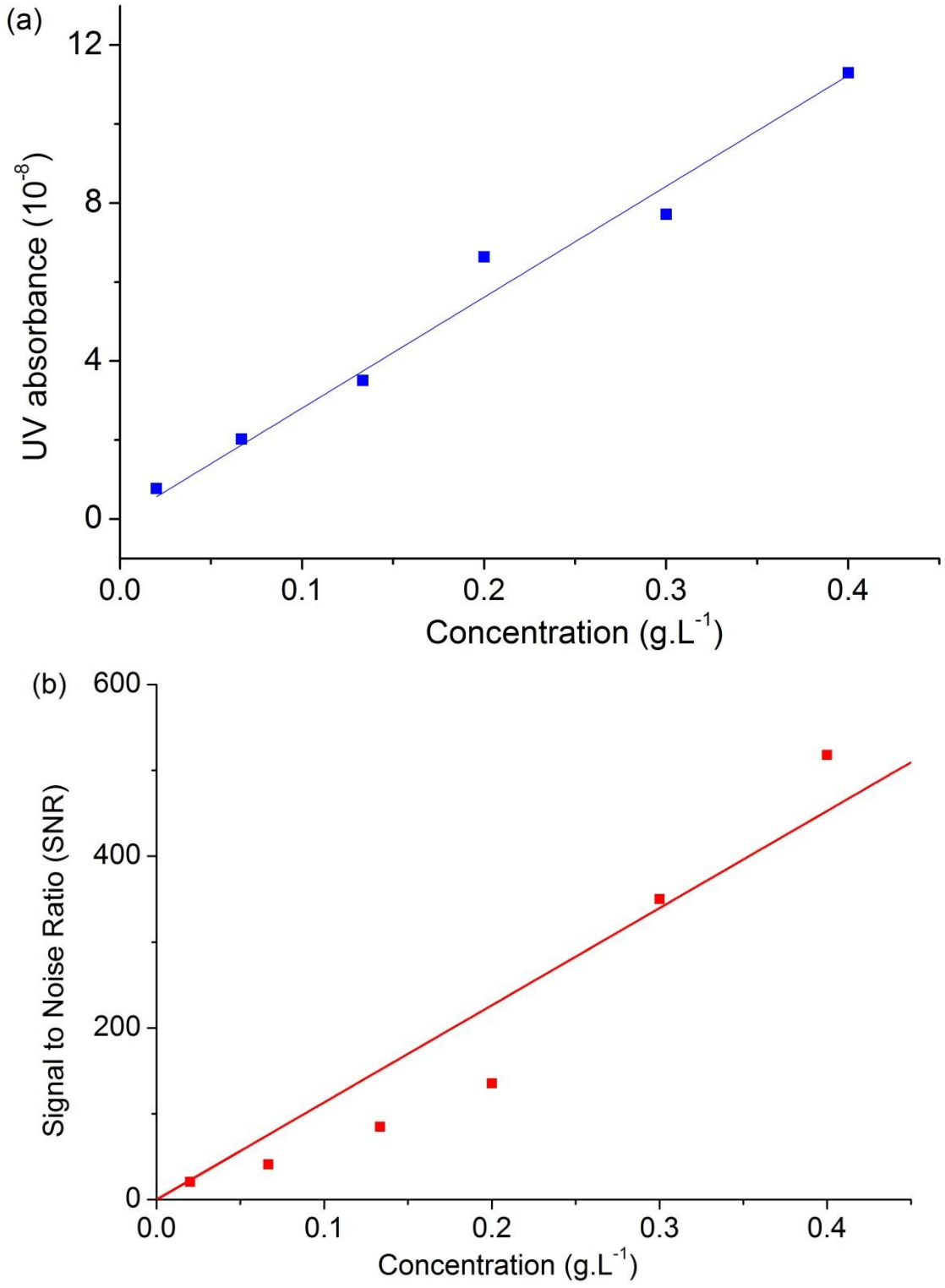


**Fig S-7** Calibration curves for (a) UV absorbance (abs) vs RGDS concentration: abs=$2.81\times10^{-7}$*concentration ($R^2$=0.992) and (b) Signal to Noise Ratio (SNR) vs RGDS concentration: SNR=1132*concentration ($R^2$=0.948)

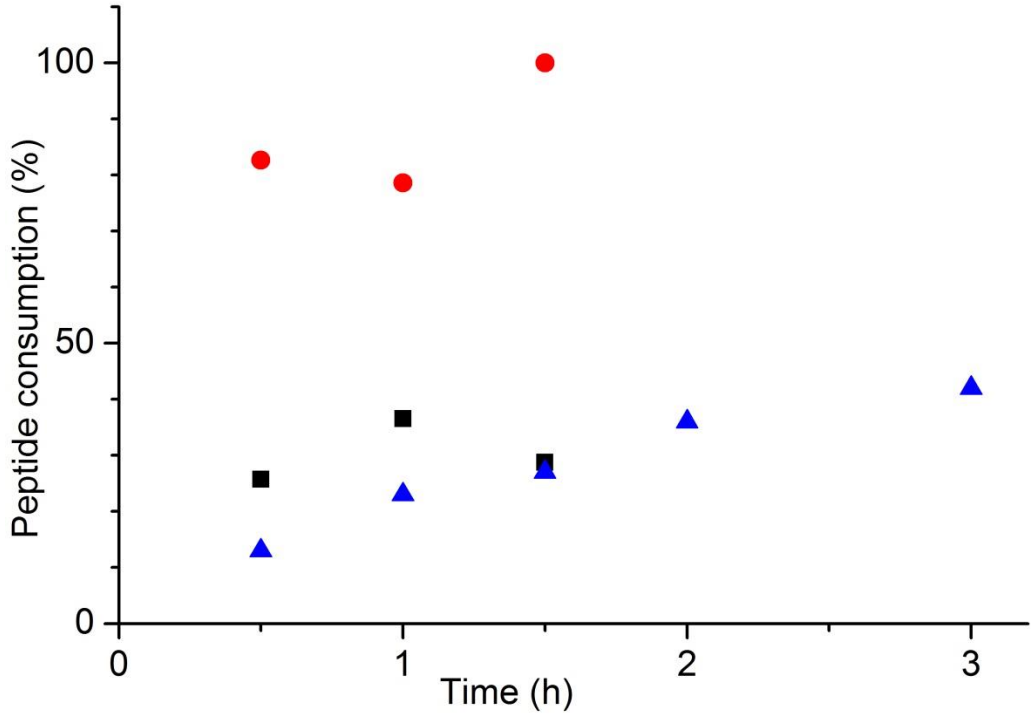


**Fig. S-8** Monitoring grafting not in real time: data for Grafted-2h (black squares), Grafted-2h-d (red circle) and Grafted-3h-d (blue triangles)

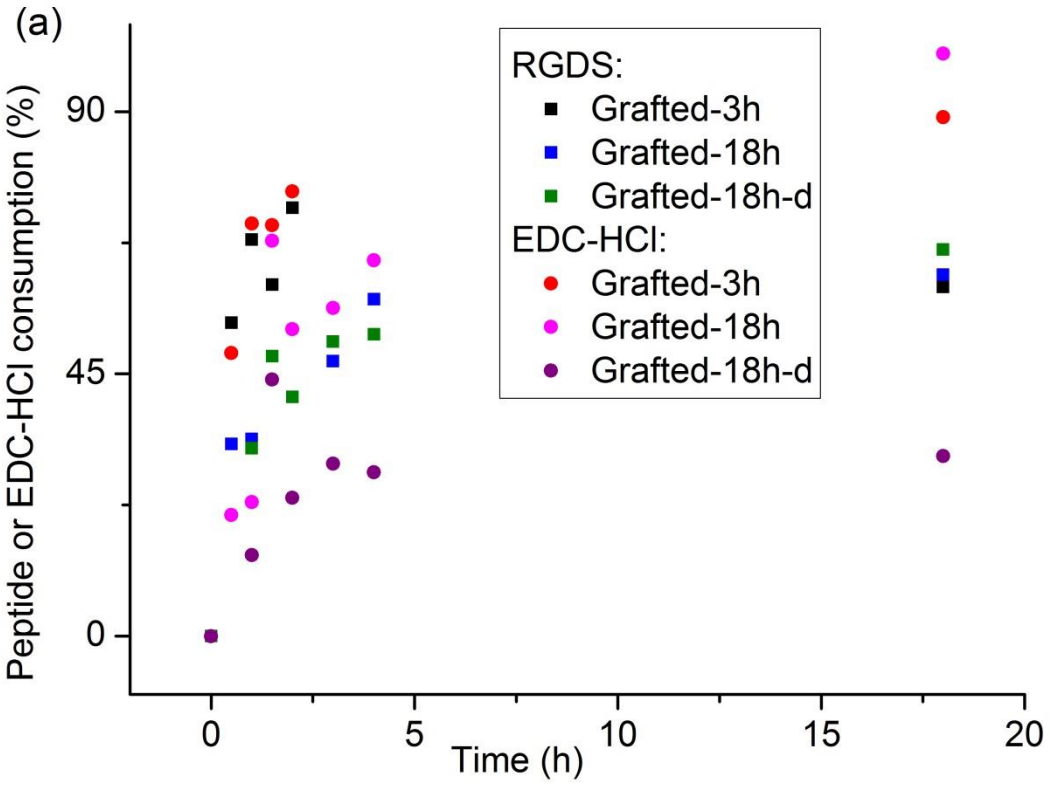

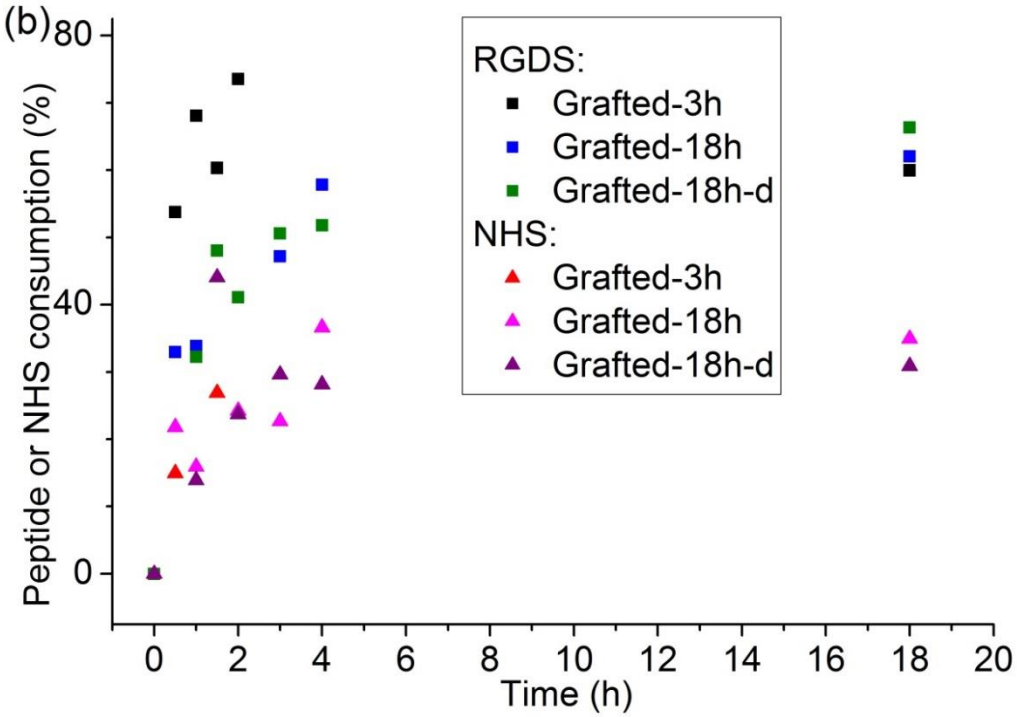


**Fig. S-9** Peptide consumption (squares) compared to a) EDC-HCl (circles) and b) NHS (triangles) consumption

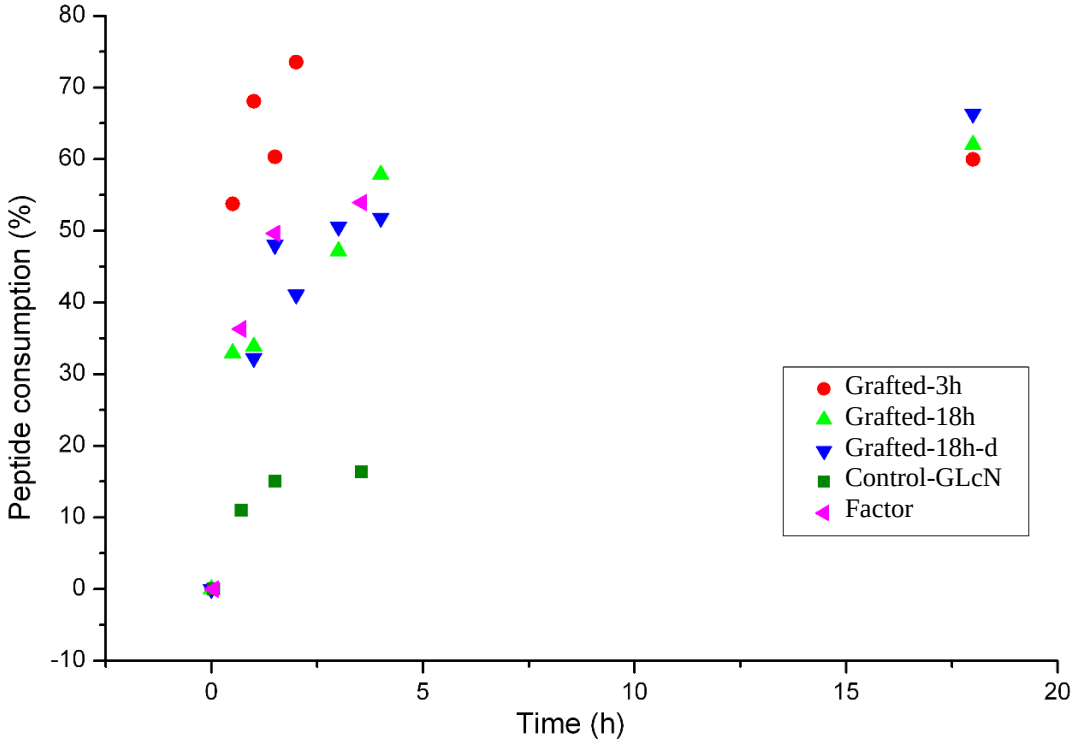


**Fig. S-10** Real-time monitoring of RGDS peptide consumption during the grafting onto chitosan films and GLcN solution with capillary electrophoresis. Factor shows the Control-GLcN data scale up by a factor 2.7 to illustrate the amount of free $NH_2$ on the chitosan films in the other grafting experiments

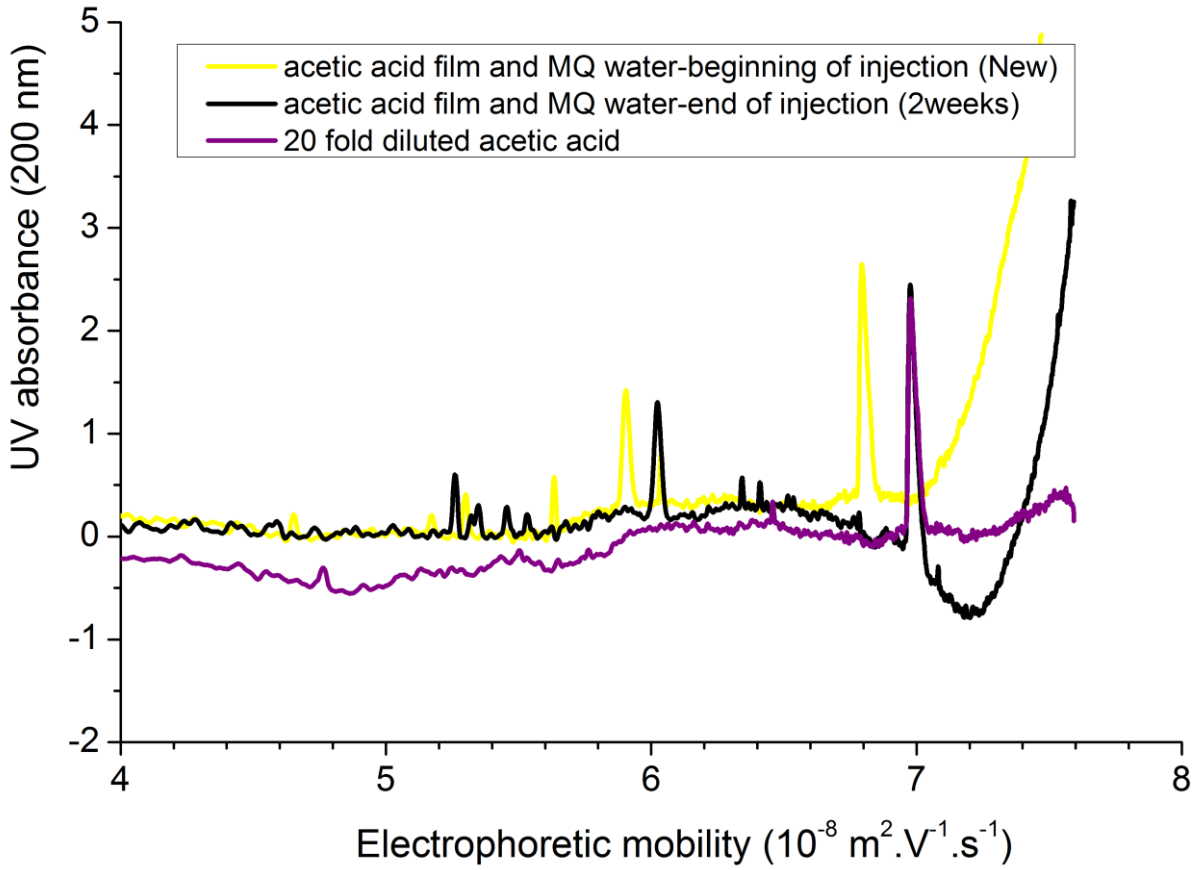


**Fig. S-11** Electropherograms of Milli-Q water exposed to a Non-treated chitosan film for a few hours and a few weeks, and of acetic acid in MilliQ water, showing the rapid leaching of acetic acid from the film placed in Milli-Q water

**Scanning Electron Microscopy (SEM)**

A JEOL JSM-6510LV scanning electron microscope was used to analyze the topography of the chitosan films before RGDS grafting. Analysis was performed using a low, 5 kV accelerating voltage to avoid charging.[2, 3] Both secondary (SEI) and backscatter (BSE) detectors were used for imaging.

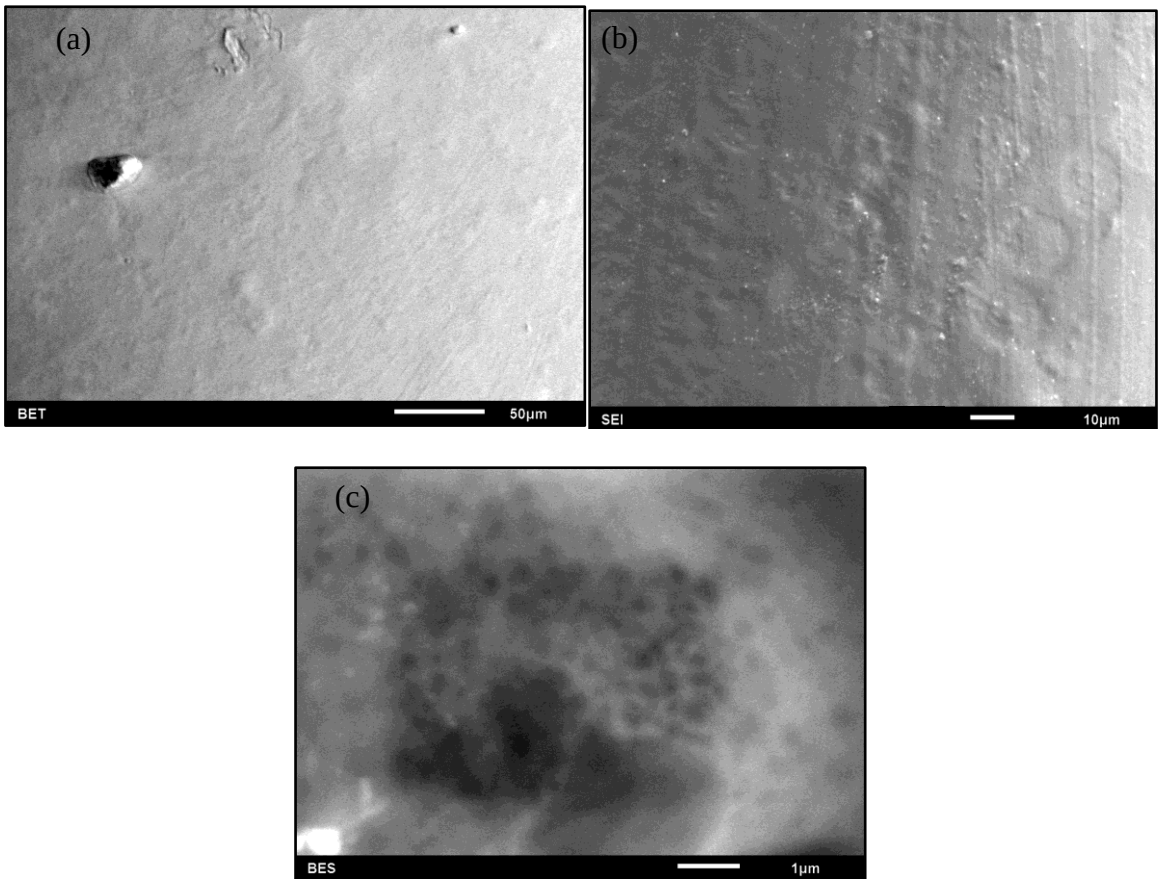


**Fig. S-12** SEM images for unmodified chitosan films. (a, b) Surface at different magnifications, and (c) beam damage to the film

**FT-IR spectroscopy**

Attenuation Total Reflectance (ATR) Fourier-Transform (FT) Infrared (IR) Spectroscopy was performed on a Perkin-Elmer Spectrum 100 FT-IR spectrometer equipped with a universal ATR sampling accessory. Spectra were acquired on the powder and films with 16 scans and a recording speed of 1 $cm^{-1}$/s.

IR spectroscopy analysis was completed on the chitosan powder and all films as shown in Fig. S-13. The spectra are in agreement with those obtained in the literature and confirm the molecular structure of chitosan.[4] There are no significant differences identified between any of the samples analyzed. RGDS grafted onto the chitosan films was not detected. The RGDS is usually detected by peaks at 1566 and 1414 $cm^{-1}$.[5] These peaks correspond to the amide II region and the carboxyl functional groups, respectively. These peaks are not apparent and are masked by the signals corresponding to the chitosan film.

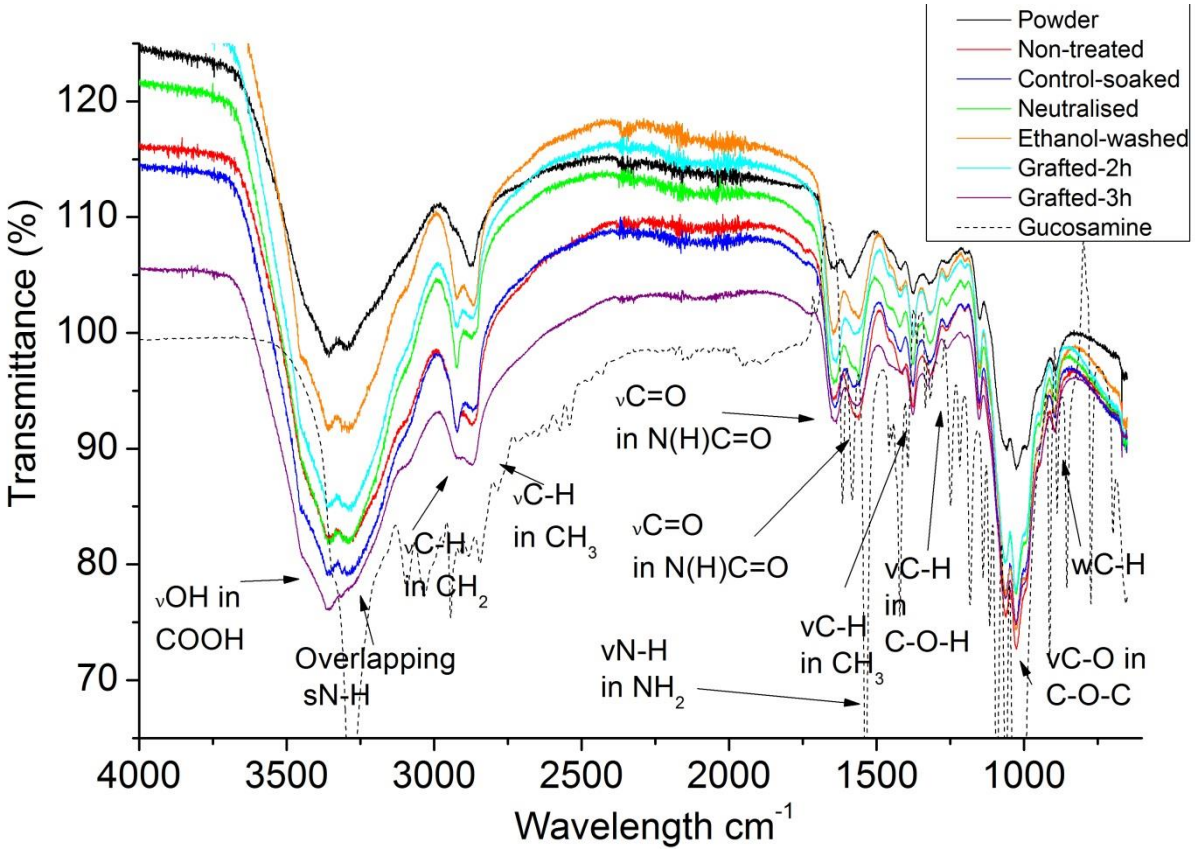


**Fig S-13** ATR –FTIR spectra of chitosan powder and film samples

**Solid-State NMR of Chitosan Films**

$^{1}$H MAS NMR spectra of all samples exhibited the expected broad signal of chitosan centered at 4.7 ppm [6]. Sample Non-treated presents a small signal superimposed on the main signal and shifted to the right, centered at 1.35 ppm (Fig. S-14). This peak was tentatively identified as acetic acid from the preparation of the chitosan film and displays a slight shift from those reported in the literature.[7] The slight shift can be accounted for by the difference in molecular packing experienced in solid-state and solution state NMR spectroscopy. Due to the low resolution of $^{1}$H NMR spectroscopy, $^{13}$C NMR spectroscopy was undertaken and was able to confirm results obtained. An extra peak not characterized as chitosan [6] was observed at a high chemical shift of 181 ppm. Similarly to the results obtained in $^{1}$H NMR spectroscopy analysis, a slight shift is observed in the acetic acid peak compared to the literature.[7] The $^{1}$H and $^{13}$C NMR spectroscopy demonstrated that the acetic acid peak disappears after simply soaking the film in PBS. The importance of rinsing the chitosan film after its production was demonstrated.

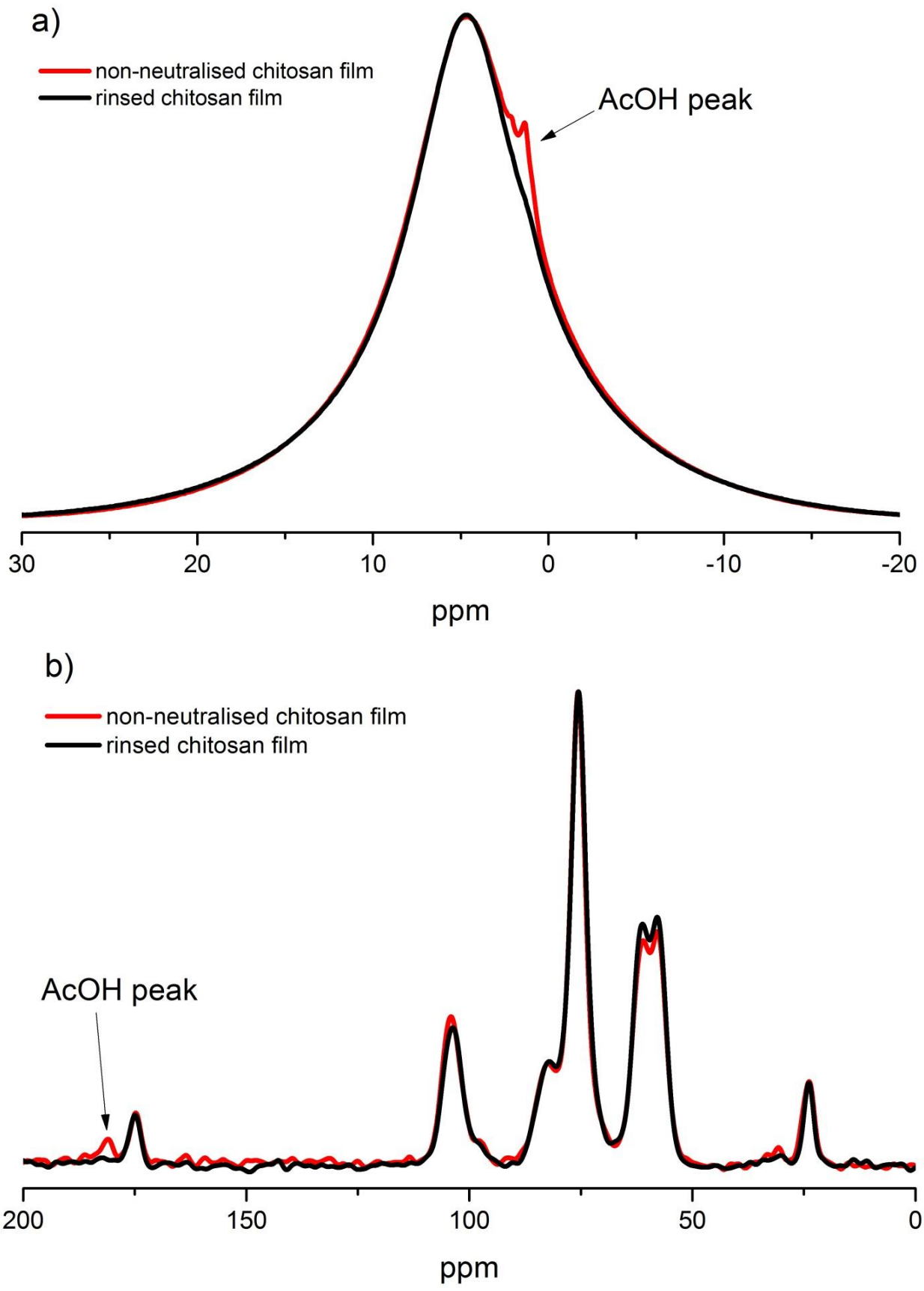


**Fig. S-14** Solid-state NMR spectra of chitosan film (Non-treated) and chitosan film rinsed with PBS (Control-soaked): $^{1}H$ MAS (a) and $^{13}C$ SPE-MAS (b)

Solid-state NMR spectroscopy analysis of the grafted films showed no indication of grafted RGDS peptide. This is illustrated in the $^{13}C$ SPE-MAS NMR spectra of Control-soaked and Graft-2a samples in Fig. S-15a and the $^{1}H$ spectra of these samples in Fig. S-15b. There is no significant difference between the spectra of the control samples and of the grafted samples. These grafting experiments were done on films not soaked in PBS and thus with films that retained acetic acid.

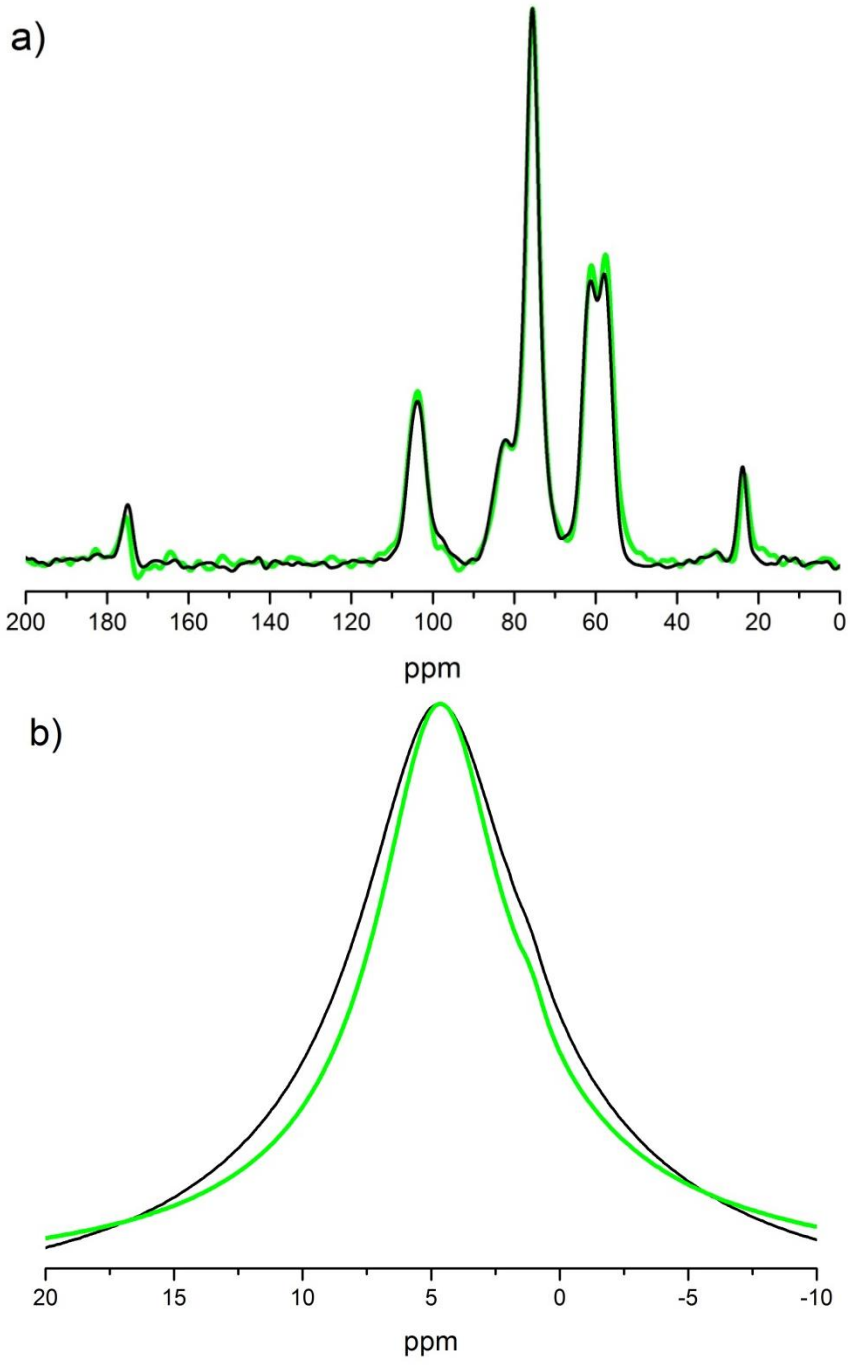

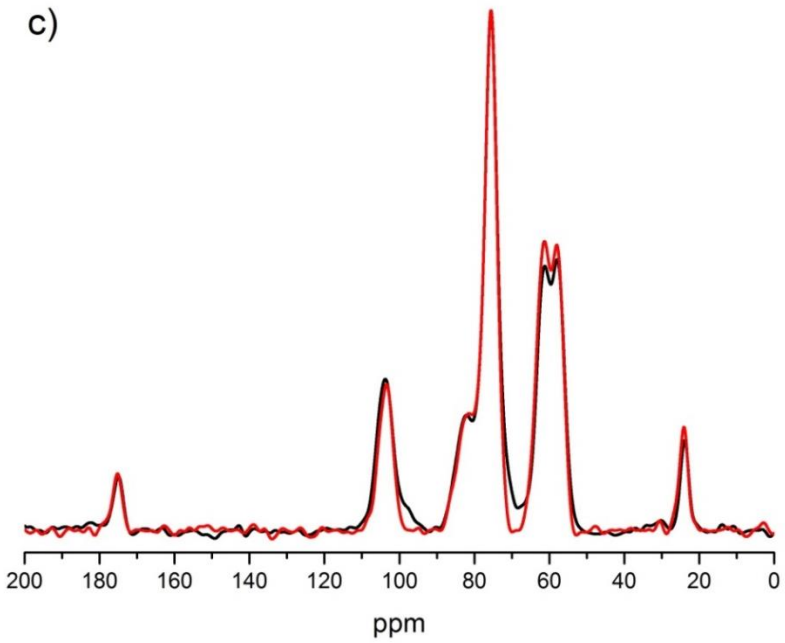


**Fig. S-15** Comparison of a) $^{13}C$ SPE-MAS NMR spectra and b) $^{1}H$ NMR spectra of Control-soaked (black line), Graft-1a (green line) and, ; c) comparison of $^{13}C$ SPE-MAS NMR spectra of Control-soaked (black line) and Graft-2a (red line)

The comparison of $^{13}C$ CP-MAS and $^{13}C$ SPE-MAS spectra reveals additional molecular dynamic information. The higher relative intensity in SPE-MAS compared to CP-MAS of C6, C8 and C9 carbons indicates a higher molecular mobility of the pending $CH_2OH$ group and of the pending acetyl group as compared to the glucose ring (Fig. S-16).

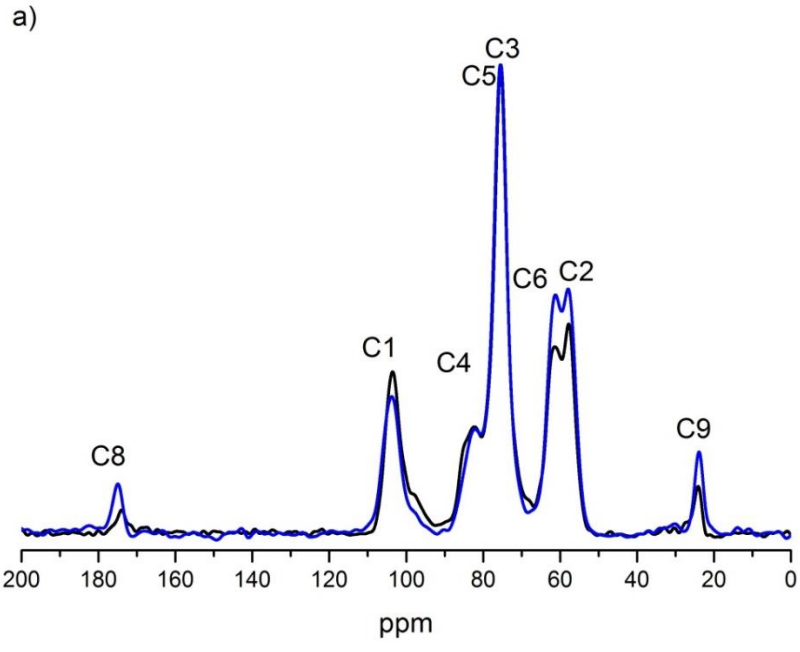

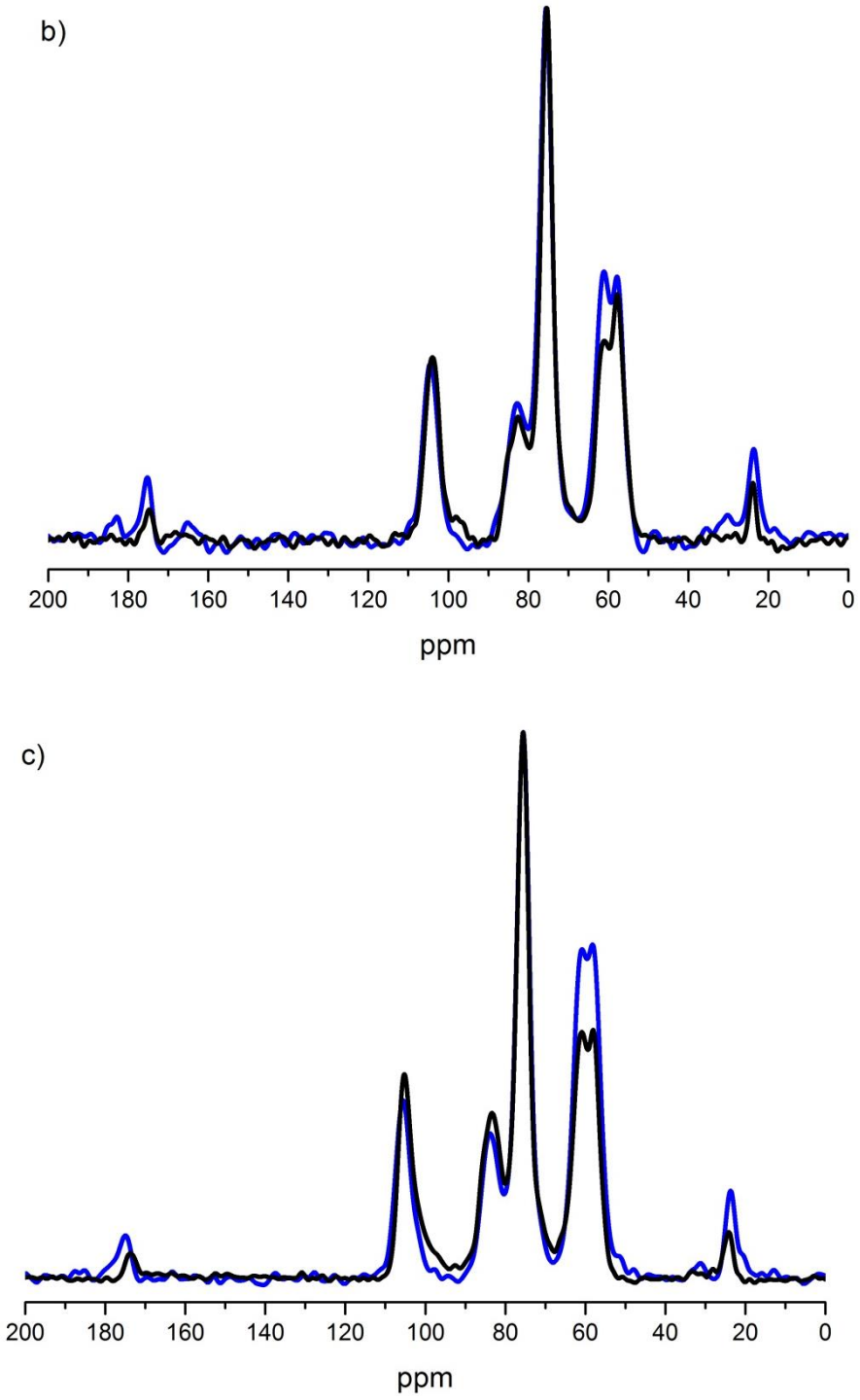


**Fig. S-16** Comparison of $^{13}C$ CP-MAS (black lines) and $^{13}C$ SPE-MAS (blue lines) NMR spectra of the a) Control-soaked film, b) Neutralized and c) Powder. The peak assignment of chitosan corresponds to the numbers shown in Fig. S-1

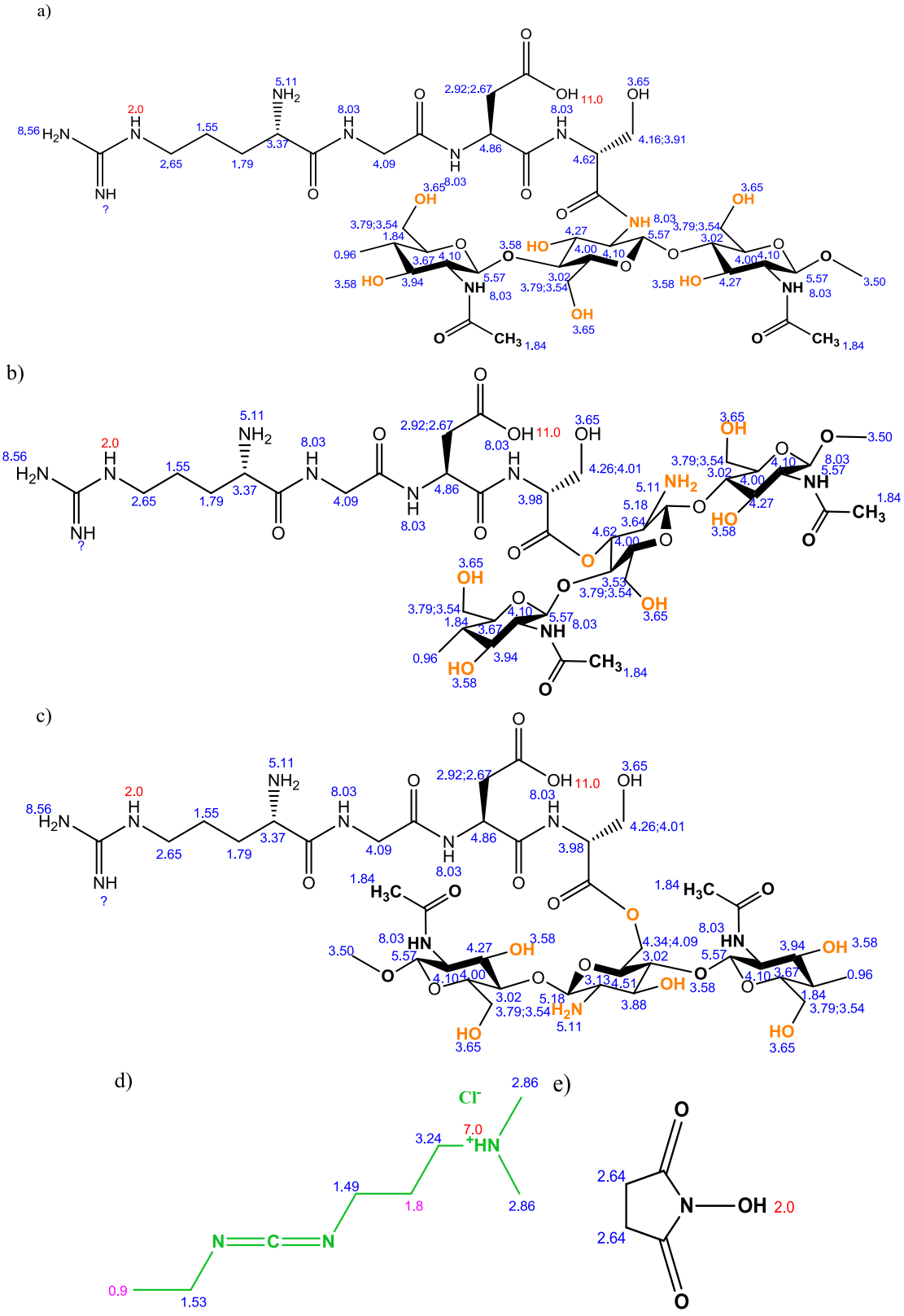


**Fig. S-17** ChemNMR estimations of $^{1}$H NMR chemical shifts of RGDS grafted to a) at an amine group of chitosan, b) at a secondary alcohol group of chitosan and c) at a primary alcohol group of the chitosan, and of d) EDC-HCl and e) NHS

a)

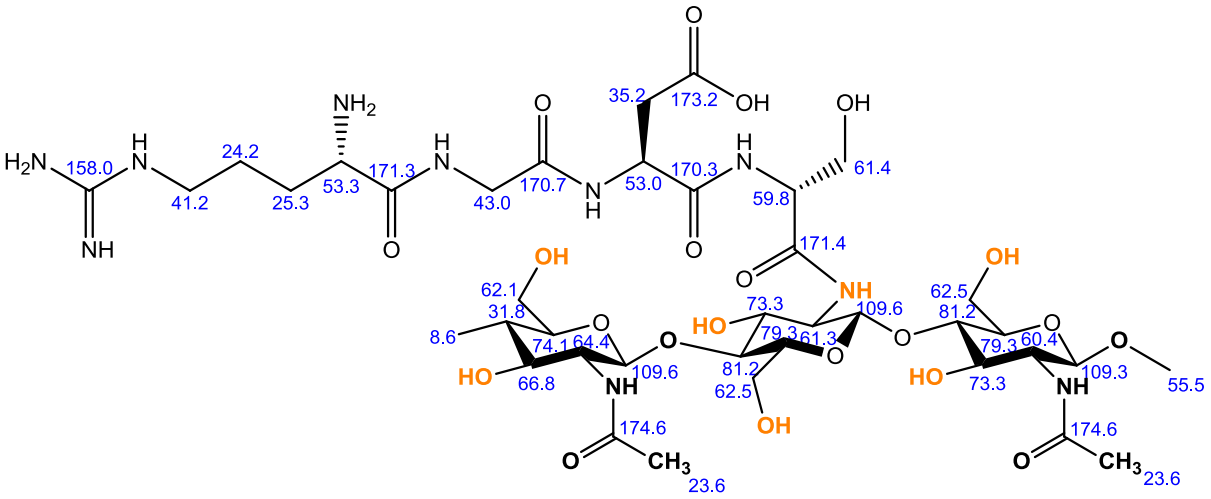

b)

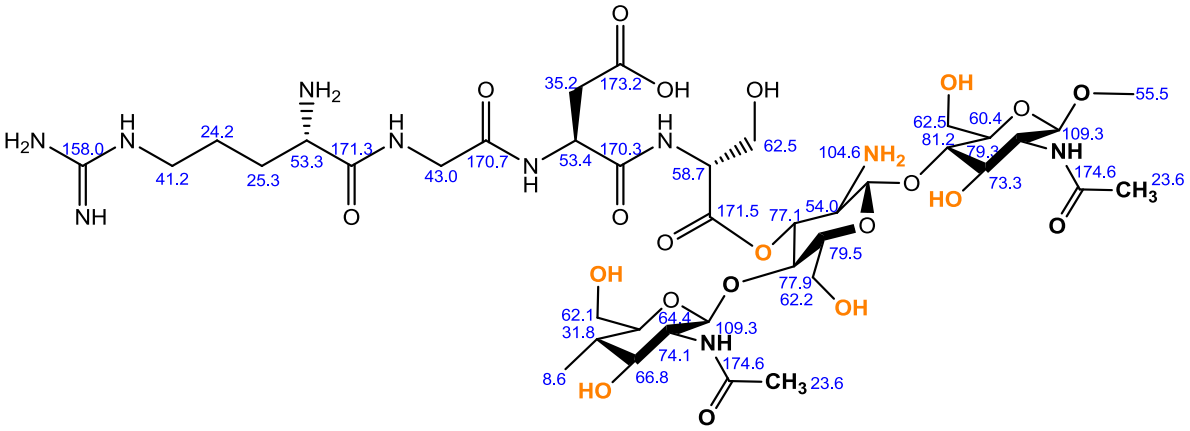

c)

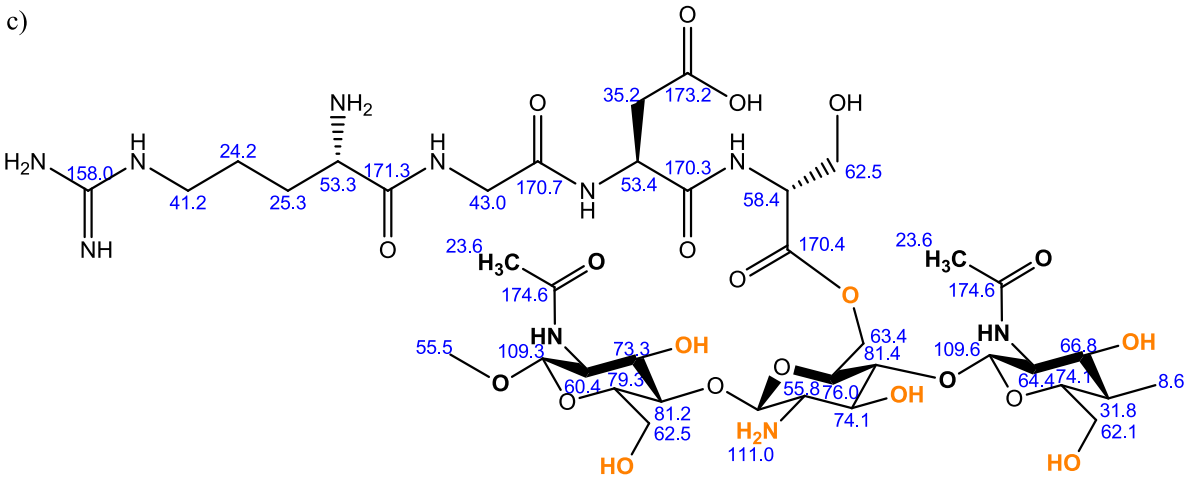

d)

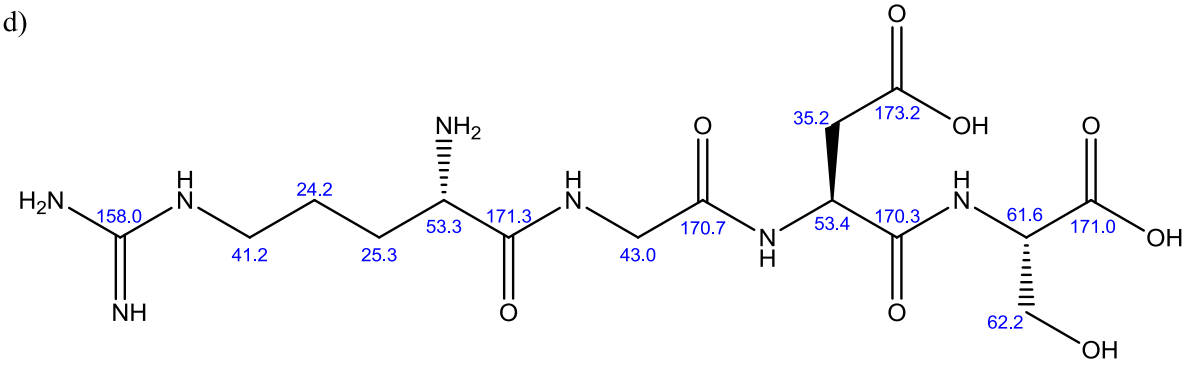

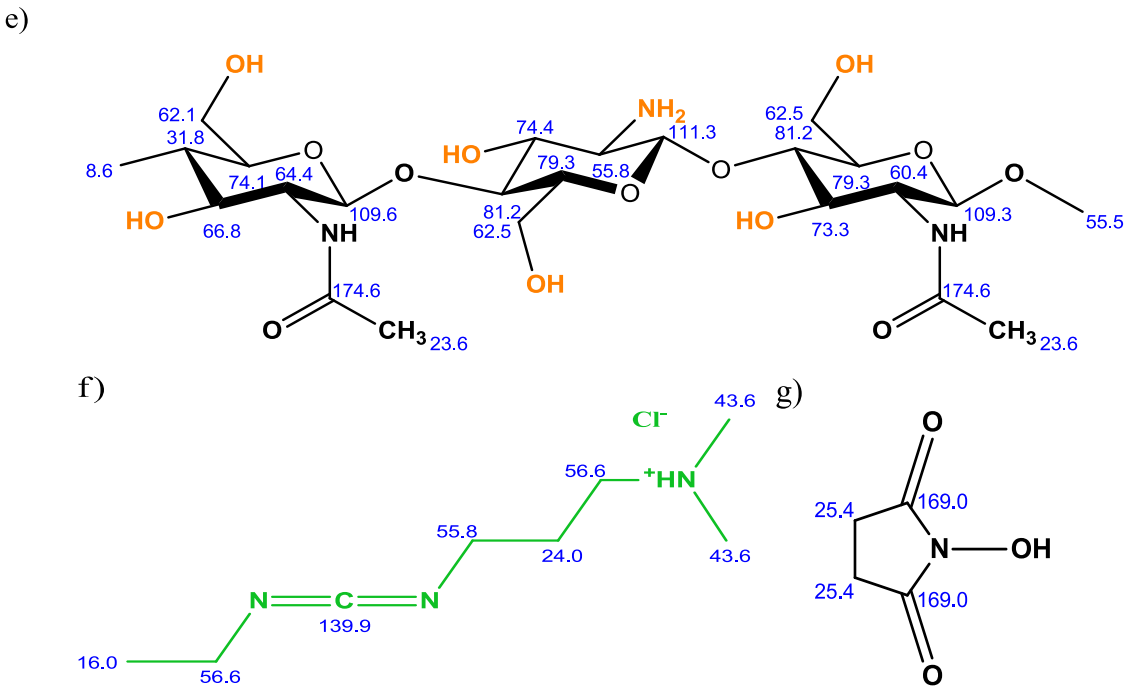


**Fig. S-18** ChemNMR estimations of $^{13}C$ NMR chemical shifts of RGDS grafted to a) at an amine group of chitosan, b) at a secondary alcohol group of chitosan, c) at a primary alcohol group of chitosan, d) non-grafted RGDS, and e) chitosan, f) EDC-HCl and g) NHS

## References


1. Moshnikova AB, Afanasyev VN, Proussakova OV, Chernyshov S, Gogvadze V, Beletsky IP (2006) Cytotoxic activity of 1-ethyl-3-(3-dimethylaminopropyl)-carbodiimide is underlain by DNA interchain cross-linking. Cell. Mol. Life Sci. 63:229-234
2. Park SI, Daeschel MA, Zhao Y (2004) Functional Properties of Antimicrobial Lysozyme-Chitosan Composite Films. J. Food Sci. 69:M215-M221
3. Pinotti A, García MA, Martino MN, Zaritzky NE (2007) Study on microstructure and physical properties of composite films based on chitosan and methylcellulose. Food Hydrocoll. 21:66-72
4. Silva SML, Braga CRC, Fook MVL, Raposo CMO, Carvalho LH, Canedo EL (2012) Application of Infrared Spectroscopy to Analysis of Chitosan/Clay Nanocomposites. In: T. Theophile, (Ed.), Materials Science, Engineering and Technology, InTech, Rijeka.
5. Karakecili AG, Gumusderelioglu M (2008) Physico-chemical and thermodynamic aspects of fibroblastic attachment on RGDS-modified chitosan membranes. Coll. Surf. B Biointerf. 61:216-223
6. Gartner C, Lopez BL, Sierra L, Graf R, Spiess HW, Gaborieau M (2011) Interplay between Structure and Dynamics in Chitosan Films Investigated with Solid-State NMR, Dynamic Mechanical Analysis, and X-ray Diffraction. Biomacromolecules 12:1380-1386
7. Gottlieb HE, Kotlyar V, Nudelman A (1997) NMR chemical shifts of common laboratory solvents as trace impurities. J. Org. Chem. 62:7512-7515